№2, 2022

ISSN 2706-977X

MATERIAL AND MECHANICAL ENGINEERING TECHNOLOGY

Editorial board of the journal

Content

DOI 10.52209/2706-977X_2022_2_3 IRSTI 53.49.07 UDC 621.785.51.062.5

Studying Steel Performance Characteristics after Gas Carburizing

Issagulova D. A.*, Naboko Ye. P., Platonova Ye. S., Yudakova V. A., Baideldinova D.D.
Abylkas Saginov Karaganda Technical University, Karaganda, Kazakhstan
*corresponding author

Abstract: The article presents the results of studying the effect of gas carburizing on the hardening of the surface layers of products made of various steel grades in order to understand the processes of destruction and wear of various products during their operation, since the service life and reliability of the product depend and are often completely determined by the state of the surface layer.

Keywords: gas carburizing, reliability, durability, thermo-chemical treatment, performance characteristics, microstructure, carburized layer, wear resistance, surface hardness, case-hardened steels.

Introduction

Taking into account the accelerated development of technology, the issues of increasing reliability and durability of machine parts, instruments, sets, the quality and efficiency of work, and consequently the issues of saving materials, combating corrosion and wear of machine parts, are becoming extremely relevant. The role of these problems in the durability of machines and mechanisms has especially increased at the present time, since the development of most industries (space, aviation, thermal power engineering, radio electronics, nuclear energy, etc.) is associated with increasing the aggressiveness of environments, temperatures, loads in which parts and sets operate. One of the solutions to these issues is hardening the surface layers of products.

The results of experimental studying the processes of destruction and wear of various products during their operation have shown that the service life and reliability of the product depend and are often completely determined by the state of the surface layer. The best way to solve the problem of increasing the quality, reliability, and durability of products is to develop modification methods that can improve several characteristics of the surface layer, such as defectiveness, roughness, redistribution of internal stresses, and remove cracked and relief layers [1-4].

There are various ways of changing the surface properties of products. One such method is changing the composition of the metal surface, in which the surface layers are subjected to diffusion thermo-chemical treatment (TCT), which results in the formation of a new alloy that is different from the core, on the surface of the product. With the use of TCT, it is possible to obtain an alloy of almost any composition in the surface layer of the product and therefore, to provide a set of necessary properties: physical, chemical, mechanical, and others. One of the most common TCT methods is carburizing.

1. Methodology

There was studied the gas carburizing effect on performance characteristics on the example of four steel grades: 3, 20, 20H2N4A и 12H18N9T (theor chemical composition is given in Table 1 [5]).

Table 1. Steel chemical composition

Steel	Element content, %						
	C	Si	Mn	Cr	Ni	S	P
3	0.14–0.22	0.05–0.17	0.4–0.65	0.3	0.3	0.05	0.04
20	0.17–0.24	0.1	0.3–0.65	0.25	0.25	0.04	0.035
20H2N4A	0.16–0.22	0.17–0.37	0.3–0.6	1.25–1.65	3.25–3.65	0.025	0.025
12H18NH9T	0.12	0.8	2.0	17.0–19.0	8.0–9.5	0.025	0.035

When carburizing alloyed steels, the susceptibility to cracking depends on the cooling mode. During thermo-chemical treatment cracks of all types occur due to internal stresses. These stresses are caused by the heterogeneity of various zones of the cemented layer structure, which is inherent in its very nature. In alloyed steels, as a result of cooling after carburizing, zones with the structure of troostite, martensite, and retained austenite can form in the layer that have different specific volumes, which causes the occurrence of internal stresses. The essence of all recommendations for the prevention of cracks associated with structural transformations in the carburized layer is to avoid the occurrence of a streaky structure in it that consists of zones with different specific volumes. Each steel grade has its own "dangerous" cooling rate, which contributes to the formation of the most inhomogeneous structure and can cause cracks. To prevent cracks, cooling must be accelerated or slowed down depending on the steel grade, the type of parts and other conditions [6 - 8].

For impact bending tests, samples were made according to GOST 9454–78 (type 11). The shape and dimensions of the test samples were selected from Table 2.

Table 2. The shape and dimensions of the test samples

Concentrator type	Concentrator radius R, mm	Sample type	Length L, mm	Width B, mm	height H, mm	Effective section height H_1, mm
V	0.25±0.025	11	55±0.6	10±0.1	10±0.1	8±0.05
		12		7.5±0.1		
		13		5±0.05		
		14		2±0.05	8±0.1	6±0.05

Based on the analysis of the literature data there were proposed sample thermo-chemical treatment modes (Table 3).

Table 3. Modes of steel carburizing and thermo-chemical treatment

Mode No.	Carburizing temperature, °C	Carburizing duration, hours	Quenching temperature, °C	Cooling medium	Tempering temperature, °C	Cooling medium
1	910±10	5	800±10	oil	200±10	air
2	950±10	10	840±10	oil	200±10	air
3	900±10	10	780-800	oil	180±10	air

When carburizing, as in other types of TCT, several processes occur simultaneously:

1) formation in the environment (or in a separate reaction volume) of a diffusing element in the atomic (ionized) state (thermal dissociation);

2) adsorption ("sticking") of atoms (ions) on the metal surface with the formation of chemical bonds between the ions of the saturating element and the base metal;

3) diffusion of adsorbed atoms from the surface into the depth of the treated metal (product). The thermodynamic driving force of diffusion is the difference in concentration of the diffusing element. As a result of these processes, the chemical composition of the surface layer changes, and a concentration gradient of the saturating element is formed in the surface and underlying layers. The concentration of the diffusing element decreases from the surface to the depth of the metal. As a result, the structure and properties of steel change.

After slow cooling, the following zones can be distinguished in the structure of the carburized layer (from the surface to the core):

1) a hypereutectoid zone consisting of perlite and secondary cementite forming a network along the former austenite grain;

2) an eutectoid zone consisting of one lamellar perlite,

3, 4) a hypoeutectoid zone consisting of perlite and ferrite.

The core will have the structure of the original (before carburizing) steel. Thus, by studying the structure of case-hardened steel after slow cooling, one can determine the depth of carburization. The technical depth of carbutizing is often taken as the distance from the surface to the zone where the carbon concentration is 0.4%, i.e. the structure consists of 50% pearlite and 50% ferrite. The carburizing depth depending on the purpose of the product and the composition of the steel, is usually in the range of 0.5-2.0 mm. At this the concentration of carbon in the surface layer of the product is 0.8-1.0% [9 - 11].

2. Results and discussion

The performance properties of case-hardened steels depend not only on the properties and structure of the carburized layer but also on the properties of the part core. Insufficient strength of the core and the zone of retained austenite can lead to deformation of the sublayer zone when the load is applied, to increasing internal stresses in the layer and its destruction. With decreasing the difference in the carbon content in the base and in the surface layer, the difference in changing the specific volume of the carburized layer and the core decreases and the level of compressive stresses in the layer decreases. However, excessive hardening of the core reduces its endurance limit, crack resistance and toughness of ccase-hardened products.

In the initial state after carburizing and high tempering with cooling in air, the basis of the structure of the 20H2N4A steel layer is the lamellar component of the troostite type (Figure 1). In addition, after carburizing due to prolonged holding at high temperatures, steels become coarse-grained.

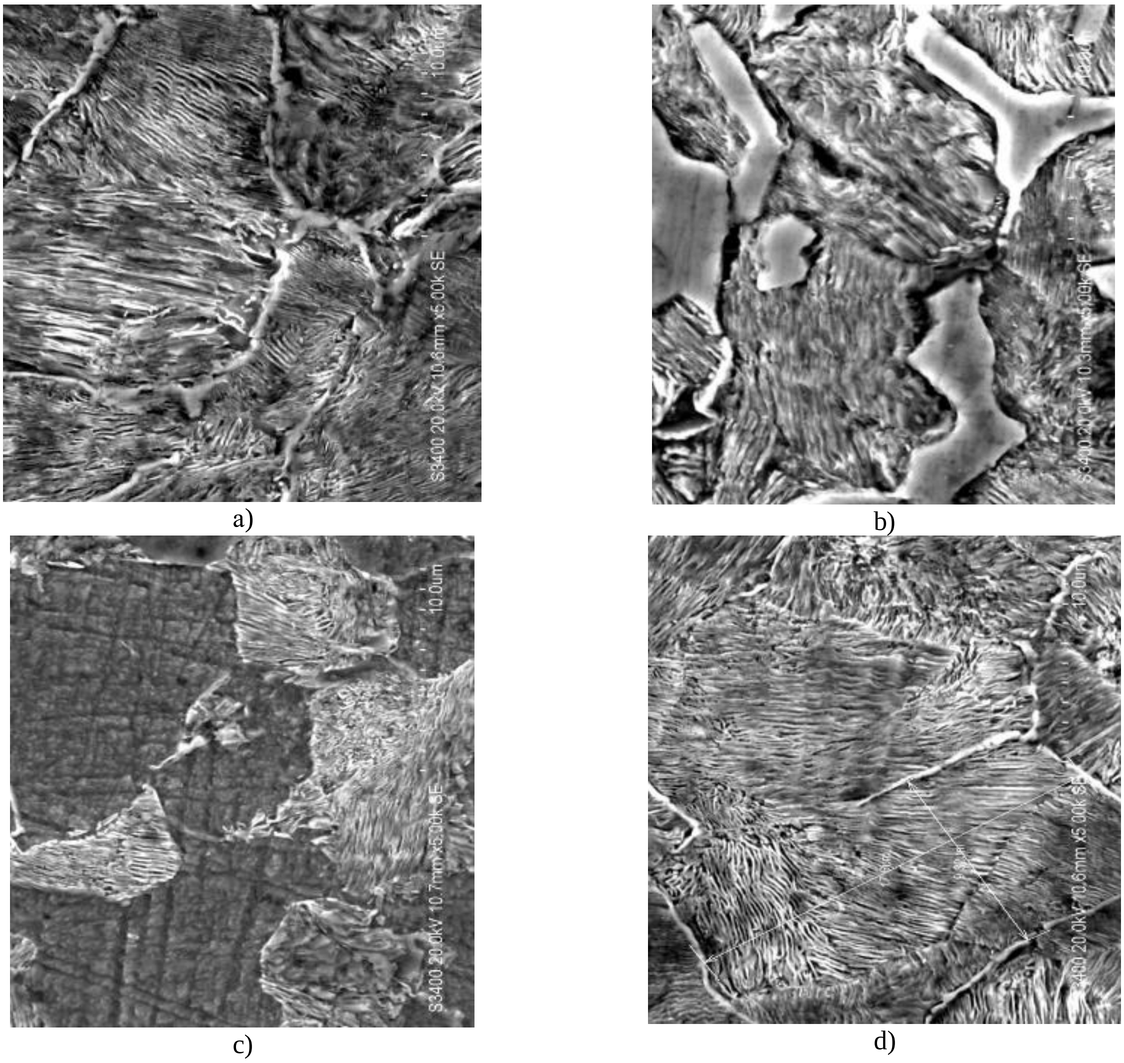

Fig. 1. Microstructure of the carburized layer ×5000, steel 20H2N4A: Distance from the surface, mm: a - 0.04; b - 0.12; c – 0.27; d - 1.50

The structure of the carburized layer after the final heat treatment is a martensitic-austenitic mixture strengthened with uniformly distributed dispersed carbides, the amount of which decreases with increasing the distance from the surface (Figure 2). The structure of the steel base is represented by packages of martensitic plates of different orientation inherited from the orientation of the initial austenite grain.

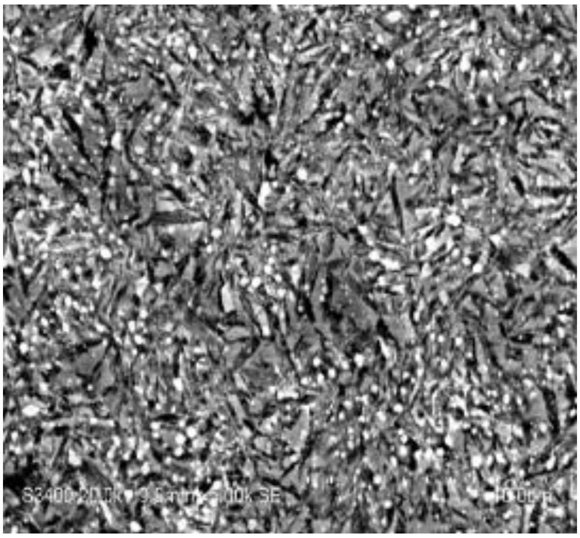

Fig.2. Microstructure of the carburized layer of steel 20H2N4A after heat treatment × 5000, distance from the surface 0.06 mm

The surface hardness of the carburized 20H2N4A layer is in the range of HRC ~ 58-62 and in the core HRC ~ 30-45. During carburizing not the total but the effective thickness of the layer is often controlled. The effective thickness corresponds to the layer zone from the saturation surface to the boundary of the zone with hardness of HRC ~50. The thickness of the effective layer is 0.4-1.8 mm.

Table 4 shows the surface hardness values of the samples after gas carburizing and full heat treatment.

Table 4. Surface hardness of samples

Steel	3	20	20H2N4A	12H18N9T
Hardness, HRC	45 - 47	37 - 42	58 - 62	10 - 12

Conclusions

The tests carried out have shown the following results: the hardness of the hardened layer after carburizing on samples of steel 20H2N4A has the maximum result of 58-62 HRC, the hardness of hardened samples after gas carburizing of steel 12H18N9T did not change. The tensile tests have shown that the samples have extremely high tensile strength (for example, after calculations, the tensile strength of the sample of steel 20H2N4A is equal to 1267.38 N/mm^2, and the tensile strength for steel 40H after quenching at 850°C in water and tempering at the temperature of 200°C (which corresponds to the hardness of 55 HRC) is 1760 N/mm^2). The samples made of corrosion-resistant steel 12H18N9T have shown that carburizing does not lead to changing the performance properties for this steel grade, since they have low hardness and strength; the products made of special case-hardened steel 20H2N4A are able to withstand significant shock loads and to provide the required strength and hardness with satisfactory toughness. After gas carburizing and hardening, the surface layer of 20H2N4A steel, in comparison with steels 3 and 20, is more resistant to wear, reliable and durable due to the presence of chromium and nickel in the chemical composition, which increase the strength properties and reduce the tendency to brittle fracture.

The studies carried out allow concluding that the performance characteristics obtained after gas carburizing will correspond to materials that possess the ability to withstand impact loads, high hardness after hardening, wear resistance and contact endurance, which solves the problems of ensuring reliability and durability of machines and mechanisms.

References

[1] Kalner V.D., Nikonov V.F., Yurassov S.A. Modern technology of gas carburizing and nitrogas carburizing //Metal Science and Thermal Processing of Metal, № 9, 1973. - P. 23 – 26.
[2] Assonov A.D. Gas carburizing with induction heating: textbook. - M: Mashgiz, 1958. - 90 p.
[3] Zhetessova G., Zharkevich O., Platonova Ye. Building mathematical model for gas-thermal process of coating evaporation //Časopis Metalurgija, № 1, 2016. - P.63 - 66.
[4] Yeremin N., Yurov V., Platonova Ye. Evaluating the Corrosion Resistance of Multi-Element Metal Coatings //AIP Conference Proceedings 1876, 020073, 2017. – P. 123 – 125.
[5] Lyakhovich L.S. Chemical-thermal treatment of metals and alloys: a reference book. - M.: Metallurgiya, 1981. - 424 p.
[6] Rudenko S.P., Valko A.L., Mossunov E.I. The structure of carburized layers of gears of transmissions of energy-saturated machines //Metal Science and Thermal Processing of Metals, №. 4, 2012. - P. 38 – 42.
[7] Shcherbakova Ye..P., Kvon Sv.S., Issagulova D.A., Arinova S.K. Heat treatment effect on the properties of vibration treated steel during crystallization //Metalurgija, Vol. 59, No. 4, 2020. - P. 493-495.

[8] Ryzhov N.M., Semenov M.Yu. Wear resistance of a carburized layer of alloy steel with an excess carbide phase. //Friction and Wear, V.T. 19, 1998. - P. 235 – 240.
[9] Schastlivtsev V.M., Kaletina Yu.V., Fokina E.A. (). Residual austenite in alloyed steels. – Yekaterinburg: EGTU, 2014. - 236 p.
[10] Kulikov V.Yu., Ibatov M.K., Kvon Sv.S., Issagulova D.A. (). Studying the properties of shell molds manufactured under industrial conditions using unsteady-state pressure //Metalurgija, Vol. 59, № 4, 2020. - p. 499-502.

Information of the authors

Issagulova Diana Aristotelevna, PhD, acting associate professor of the department "Nanotechnologies and metallurgy" of Abylkas Saginov Karaganda Technical University
E-mail: isagulovada@mail.ru

Naboko Yelena Petrovna, candidate of technical sciences, associate professor of the department "Nanotechnologies and metallurgy" of Abylkas Saginov Karaganda Technical University
E-mail: lena_nep@mail.ru

Platonova Yelena Sergeevna, senior teacher of the department "Nanotechnologies and metallurgy" of Abylkas Saginov Karaganda Technical University
E-mail: danilina1969@list.ru

Yudakova Valeria Alexandrovna, senior teacher of the department "Nanotechnologies and metallurgy" of Abylkas Saginov Karaganda Technical University
E-mail:lera-mlp@mail.ru

Baideldinova Diana Daurenkyzy, master student of the department "Nanotechnologies and metallurgy" of Abylkas Saginov Karaganda Technical University
E-mail: baideldinova.dd@kaz-metiz.com

DOI 10.52209/2706-977X_2022_2_8 IRSTI 55.53.01 UDC 621.01:929.6

The Impact of Engineering and Technical Achievements on the Formation of National Symbols of the States of the Modern World - on the Translation of the Review of State Coats of Arms

Mayer R.[1], Warguła Ł.[2*]
[1] Complex of commercial schools named after the Heroes of the Poznań June '56 in Poznań, Poland
[2] Poznan University of Technology, Poland,
*corresponding author

Annotation. The United Nations in its list of states includes 193 states. Each of them is characterized by a different national symbolism. One of the main symbols of each state is the coat of arms. The coat of arms may contain important symbols of the state, such as historical figures, geographical areas, vegetation, animals, religious symbols, etc. The aim of this article is to present engineering and technical achievements that are depicted on one of the most important symbols of the nation (state coat of arms). Among these achievements, the most popular symbols are weapons 30%, ships and boats 10%, agricultural equipment 6% and aspects of mechanical engineering 4%, manifested in gear symbols. Other engineering and technical achievements include instruments 3%, measuring devices (weight) 2%, power plants 1.5%, buildings of the mining and production industry 1%. The review included the coats of arms of the countries of the modern world that are members of the United Nations in 2022. It can be seen that for over a third of the countries of the modern world, engineering and technical achievements are an important state symbol, honored with being placed on the state coat of arms.

Key words: state symbol, mechanical engineering, toothed gear, power station, ship, weapon.

Introduction

The state emblem is understood as a graphic symbol that is a symbol of the state, usually referring to the historical tradition of a given state (nation). This graphic sign together with the heraldic shield is the coat of arms of the state [1]. The coat of arms of the state is a symbol that represents the state. It is considered one of the most important signs of the sovereignty of a given political entity. Most often it is related to the history of the country [2, 3]. Many analyzes of geographical elements and their symbolism on the flags and coats of arms of the countries of the modern world have been carried out. In 2002, Wrona analyzed the graphic and color elements of state flags and coats of arms, directly or indirectly with reference to geographical sciences [4]. The author also analyzed the symbols of African [5], Asian [6, 7] and American [8] countries, taking into account heraldic, geographic, encyclopedic and other scientific and popular science [5] aspects. In 2011, Wrona analyzed the symbolism of economic activity in the coats of arms of the countries of the modern world [9], and in 2016 the religious symbolism on the flags and coats of arms of the countries of the modern world [10]. The literature on the subject shows a lack of analysis of engineering and technical symbols appearing in the coats of arms of the countries of the modern world. The article presents an overview of the coats of arms of countries in which symbols of engineering and technical achievements such as devices, machines, machine parts, tools, weapons, energy or transport structures are recognized. The aim of the article is to show that the influence of engineering and technical achievements can be seen in many state symbols around the world. Additionally, the authors analyzed which of these achievements is most often presented. The analysis did not take into account building structures other than those for technical and utility applications (buildings of religious or historical importance were not taken into account).

1. Aspects of mechanical engineering in national symbols

Mechanical engineering is one of the basic sciences closely related to the development of industry. The main effect of the work carried out in this field of science are machines and devices, but they would not have been created without machine parts. Looking at the coats of arms, you can see that gears are an important symbol of such countries as: Botswana, Angola, China, Laos, Rowanda, East Timor, Vietnam, Italy (Fig. 1 and 2). The gear symbol is found on around 4% of national coats of arms. For many modern engineers, the shape of the toothed rack of the gear is an involute (Fig. 3a), however, the first gears had a rectangular shape (Fig. 3b).

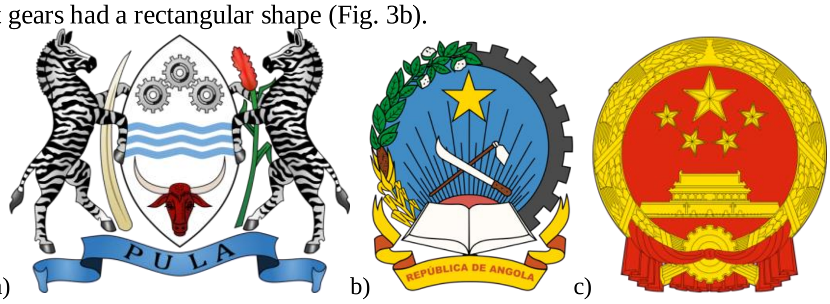

a) b) c)

Fig. 1. – Coats of arms of countries with a gear symbol: a) Botswana, b) Angola, c) China

Fig. 2. – Coats of arms of countries with a gear symbol: d) Laos, b) Rowanda, c) East Timor, d) Vietnam, e) Italy

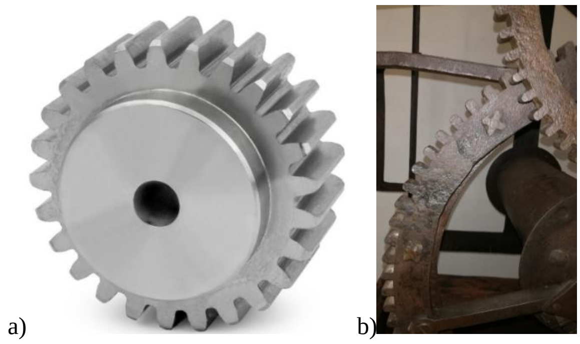

Fig. 3. – Gears: a) involute, b) rectangular (18th century - clockwork)

2. Aspects of electrical engineering in national symbols

Power plants are another engineering achievement immortalized on the coats of arms of the countries. Two types of power plants are noticed: the wind power plant (Fig. 4a) shown on the coat of arms of Ghana and the hydro power plant shown on the coat of arms of North Korea (Fig. 4b) and Laos (Fig. 4c). The first wind and water electrons were created at the end of the 19th century and are still an important achievement for human existence. The popularity of this symbol on the coats of arms of countries around the world is about 1.5% and is popular for Asia in the case of hydroelectric power plants and Africa in the case of wind farms.

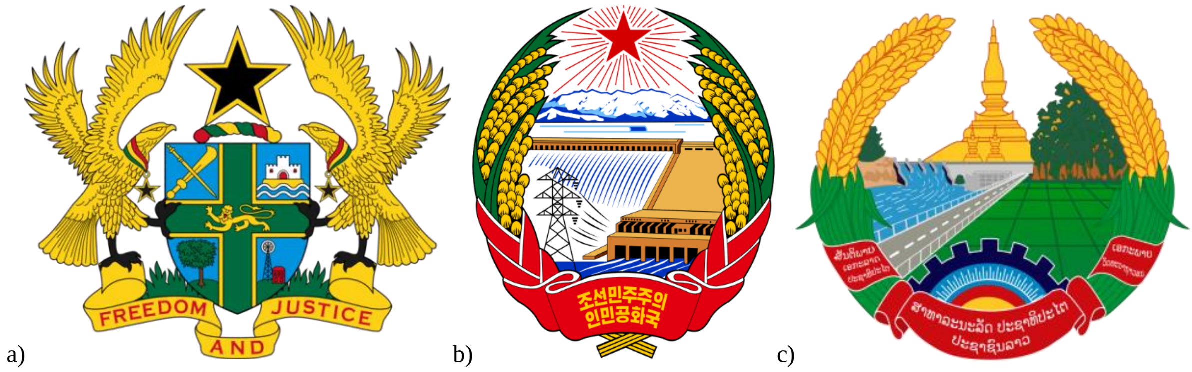

Fig. 4. – Coats of arms of countries with the symbol of a power plant: a) a wind farm on the coat of arms of Ghana, b) a hydroelectric plant on the coat of arms of North Korea, c) a hydroelectric plant on the coat of arms of Laos

3. Aspects of the manufacturing, processing and mining industries in national symbols

Many technical engineering achievements are contained in symbols representing the industry, e.g. mining (Fig. 5a) or manufacturing and processing (Fig. 5b). The coat of arms of Honduras shows elements of the mining industry, tools and mine shafts. On the other hand, the coat of arms of Algeria shows factory buildings with tall chimneys symbolizing the manufacturing and processing industry. The symbolism of the tan is about 1% of all the coats of arms of the modern world countries.

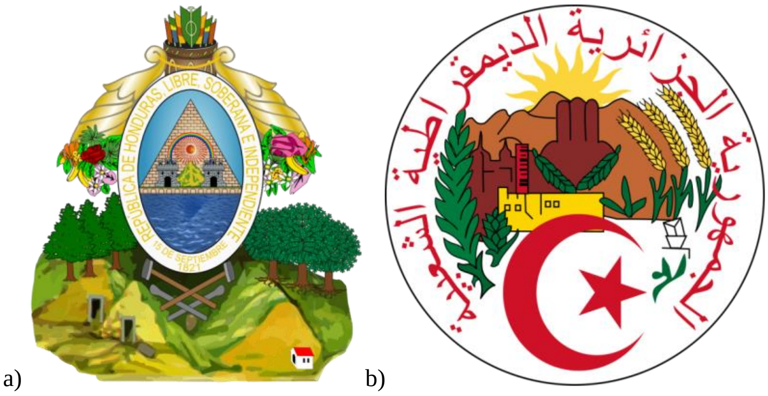

Fig. 5. – Coats of arms of countries with the symbol of industry: a) mining industry on the coat of arms of Honduras, b) production and processing industry on the coat of arms of Algeria

4. Aspects of transport engineering in national symbols

Transport, together with infrastructure structures and means of transport, is one of the symbols of technical engineering achievements, which is relatively often manifested in national symbols. We can distinguish achievements related to the construction of infrastructure: a bridge in the coat of arms of Malaysia (Fig. 6a, b) and an asphalt road on the coat of arms of Laos (Fig. 6b). Civil engineering achievements in terms of road infrastructure account for 1% of symbols in national coats of arms.

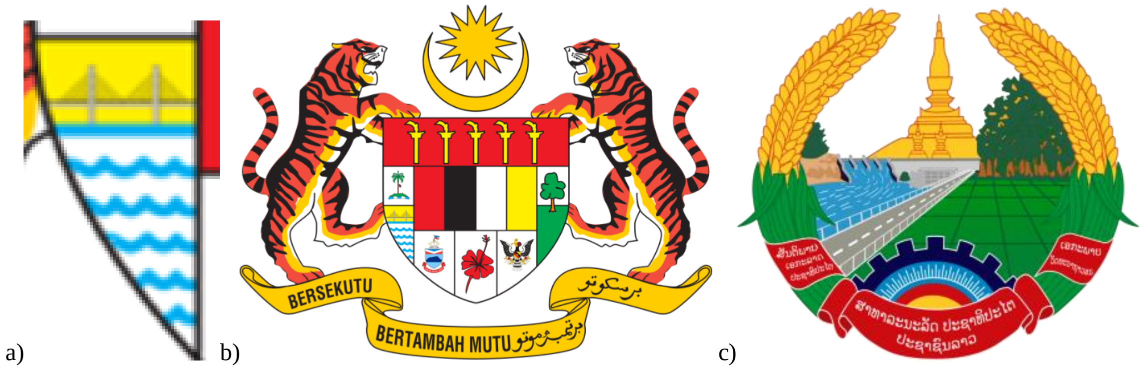

Fig. 6. – Coats of arms of countries with the symbol of transport engineering: a) bridge in the coat of arms of Malaysia, b) coat of arms of Malaysia, c) asphalt road in the coat of arms of Laos

On the other hand, means of transport in the form of ships and boats are very popular. They appear on the coats of arms of countries such as: Bahamas, Belize, Benin, Dominica, Ecuador, Fiji, Colombia, Costa Rica, Kuwait, Liberia, Mauritius, New Zealand, Gabon, Grenada, Qatar, Trinidad and Tobago, Tunisia, Saint Kitts and Nevis, Seychelles, Surinas, Marshall Islands (Fig. 7). The symbols of boats and ships account for about 10% of symbols in the coats of arms of states.

5. Agricultural engineering aspects in national symbols

The analysis of the aspects of agricultural engineering in national symbols was carried out on the example of agricultural tools. Mainly constituting hand tools for loosening the soil, spouts, shovels, plowing machines will turn, the second group of scythes, sickles and machetes for harvesting agricultural crops. Achievements of agricultural technology are visible on about 6% of national symbols, eg Liberia, Gambia, New Zealand, Tanzania, Zambia, Angola, Austria, Belize, Panama, Zimbabwe, Guyana, East Timor, Mozambique (Fig. 8).

Fig. 7. – Symbols of ships and boats in the coats of arms of: a) Bahamas, b) Belize, c) Benin, d) Dominica, e) Ecuador, f) Fiji, g) Colombia, h) Costa Rica, i) Kuwait, j) Liberia, k) Mauritius , l) New Zealand, m) Gabon, n) Grenada, o) Qatar, p) Trinidad and Tobago, r) Tunisia, s) Saint Kitts and Nevis, t) Seychelles, u) Surinam, w) Marshall Islands

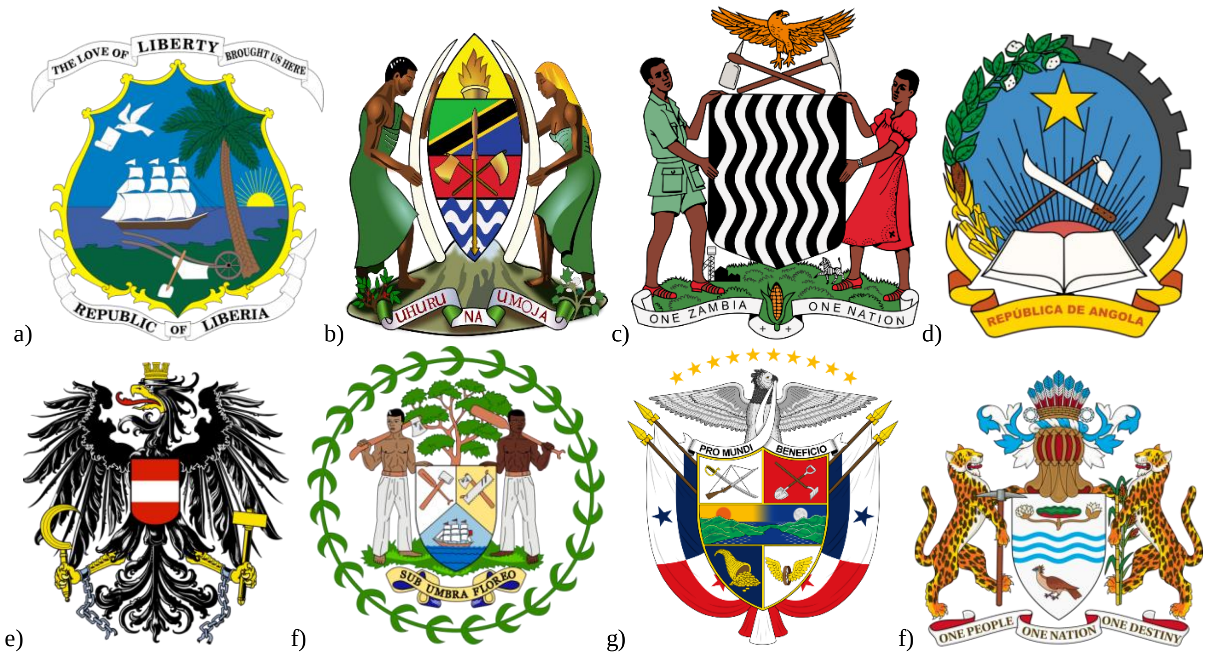

Fig. 8. – Examples of symbols of agricultural technology in the coats of arms of the state: a) Liberia, b) Tanzania, c) Zambia, d) Angola, e) Austria, f) Belize, g) Panama, f) Guyana

6. Measuring devices in national symbols

The most popular trade symbol is the weight which represents about 2% of the national symbols. This measuring device is visible on the coat of arms of countries such as Cameroon, Tunisia, Somaliland, Uruguay (Fig. 9).

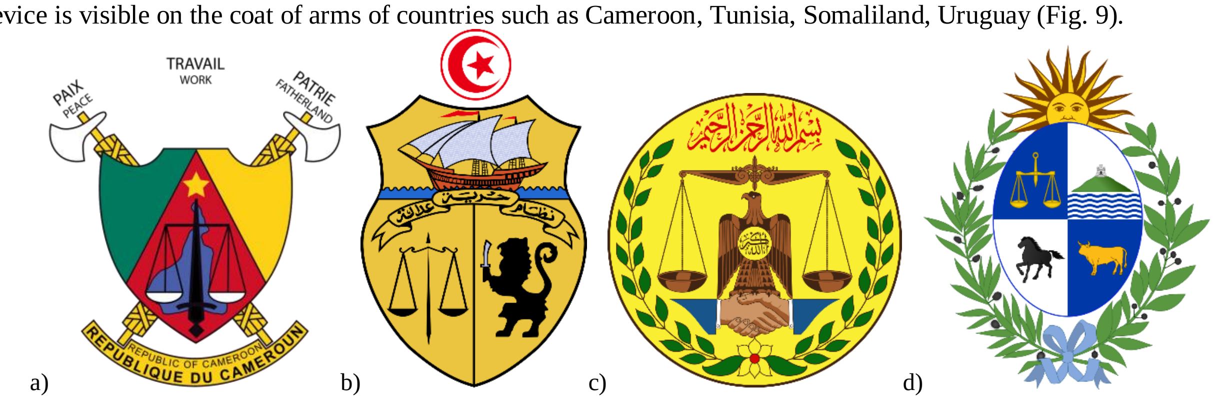

Fig. 9. – Measuring devices in the coats of arms of the following countries: a) Cameroon, b) Tunisia, c) Somaliland, d) Uruguay

7. Musical instruments in national symbols

One of the achievements of engineering is the construction of devices enabling the creation of music. Instruments are available on approximately 3% of national coats of arms. These are mainly harps, e.g. in the coat of arms of Greece, Great Britain, Canada, drums (Uganda) and blown instruments, trumpets and horns, e.g. in the coat of arms of Liechtenstein, Haiti (Fig. 10).

8. Weapons in national symbols

Weapons in national symbols have one of the most commonly used symbols in the coats of arms of the states. This technical engineering achievement is visible in almost 30% of the coats of arms of the modern world. Small arms and melee weapons are popular, including e.g. wood weapons, lances, spears, blunt weapons, mace, slashing weapons, sabers, sword, throwing weapons, bow, crossbow. Firearms, shotguns, rifles, artillery weapons, cannons are also available. There are also protective elements, e.g. shields, helmets, armor. The issue of weapons, which is a technical engineering achievement, is so popular in national symbols that it may constitute a separate article. Therefore, only selected symbols are shown in Fig. 11.

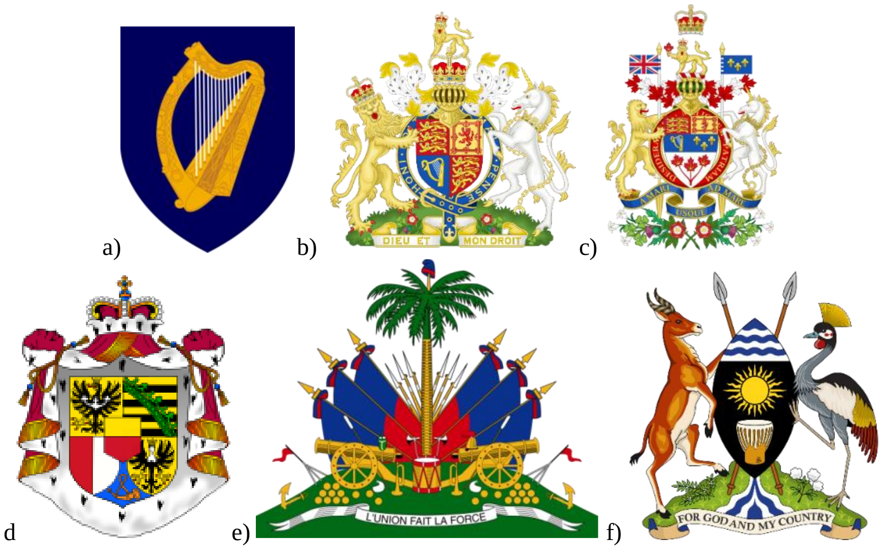

Fig. 10. – Musical instruments in the coats of arms of countries: a) Greece, b) Great Britain, c) Canada, d) Liechtenstein, e) Haiti, f) Uganda

Fig. 11. – Weapons in national coats of arms, firearms: a) East Timor, b) Mozambique, c) Western Sahara, d) Guatemala, white hand weapons: e) Vanuatu, f) Saudi Arabia, g) Djibouti, h), defensive weapons: i) Kenya, j), k) Malawi, l) Eswatini, artillery weapons: m) Haiti, throwing weapons: n) Mali, o) Jamaica.

Conclusion

Technical engineering achievements have a great influence on shaping the national identity. This phenomenon is manifested in the presentation of engineering and technical achievements in the most important symbols of the state, i.e. the state coat of arms. About 30% of the countries of the modern world show weapons in their coat of arms, it can be noticed that for many countries it is a very important symbol of shaping national identity. The second most popular engineering and technical achievement are ships and boats constitute about 10% of symbols, while symbols of land transport means (roads and bridges) account for about 1%. The third position is occupied by symbols related to technology, machines and agricultural devices (without taking into account agricultural produce) - they account for about 6%. Symbols mechanical engineering, which is the basis of many of the aforementioned achievements, appears on the coats of arms of about 4% of countries and is most often manifested by the symbol of a gear wheel. About 3% of the coats of arms of countries are musical instruments, and below 2% you can see symbols of devices used in trade (weight), the energy industry (about 1.5%) and the mining and production industry (about 1%). The political situation of the modern world in many regions is unstable, and states and their coats of arms have grown colder over the years, the current review was based on the countries belonging to the United Nations.

References

[1] Sagan S., Serzhanowa, V. Symbols of modern states (original text in Polish: Symbole państw współczesnych)// "Studia Prawnoustrojowe", No. 13, 2011. - P. 343 - 354.
[2] Dankowski M.Z. Constitutional graphic symbols of Spain and its autonomous communities //"Przegląd Prawa Konstytucyjnego, No. 6(46), 2018. - P. 341 - 359.
[3] Ylönen A. Building the nation in Southern Sudan: state emblems, symbols and national identity //Africa Review, No. 12(2), 2020. - P. 151 - 171.
[4] Wrona J. An Analysis of Geographical Elements in the Flags and Emblems of countries Around the World, and Their Symbolism (original text in Polish: Analiza elementów geograficznych i ich symboliki na flagach oraz herbach państw współczesnego świata) //"Zeszyty Naukowe/Akademia Ekonomiczna w Krakowie. Seria Specjalna, Monografie", No. 156. - 2002.
[5] Wrona J. The Appearance and Symbols Used in the Flags of Modern Central African States (original text in Polish: Wygląd i symbolika flag współczesnych państw Afryki Środkowej) //Zeszyty Naukowe/Akademia Ekonomiczna w Krakowie, No. 693, 2006. - P. 203 - 221.
[6] Wrona J. Appearance and Geographical Symbolism of the Flags and Coats of arms of Contemporary South Asian Countries //Zeszyty Naukowe, No. 746, 2007. - P. 159 - 174.
[7] Wrona J. An Analysis of the Appearance and Symbolism of Flags and Coats of Arms of the Modern States of Southeast Asia //Zeszyty Naukowe/Uniwersytet Ekonomiczny w Krakowie, No. 842, 2010. - P. 143 - 161.
[8] Wrona J. The Appearance and Geographical Symbolism of the Coats of Arms of the Modern States of South America (original text in Polish: Wygląd i geograficzna symbolika herbów współczesnych państw Ameryki Południowej)// "Zeszyty Naukowe Uniwersytetu Ekonomicznego w Krakowie",No. 917(17), 2013. - P. 109 - 125.
[9] Wrona J. Symbols of Economic Activity in the Coats of Arms of Modern Countries (original text in Polish: Symbolika działalnosci gospodarczej w herbach państw współczesnego świata) //Zeszyty Naukowe Uniwersytetu Ekonomicznego w Krakowie", No. 870(02), 2011. - P. 53 - 69.
[10] Wrona J. Religious symbols on flags and national coats of arms of states of contemporary world (original text in Polish: Symbole religijne na flagach iw herbach państw współczesnego świata) //Annales Universitatis Paedagogicae Cracoviensis Studia Geographica, No. 10, 2016. - P. 98 - 111.

Information of the authors

Mayer Roksana, student of the Complex of commercial schools named after the Heroes of the Poznań June '56 in Poznań
E-mail: roksana.mayer@gmail.com

Warguła Łukasz, PhD, associate professor of the Faculty of Mechanical Engineering of Poznan University of Technology
E-mail: lukasz.wargula@put.poznan.pl

DOI 10.52209/2706-977X_2022_2_15 IRSTI 81.09.03 UDC 666.3/7.001.24

Analysis of Research and Characteristics of Physical and Mechanical Properties of Clay Thixotropic Solutions

Kadyrov A.S., Ganyukov A.A.*, Altynbaev A.Zh.
Abylkas Saginov Karaganda Technical University, Karaganda, Kazakhstan
*corresponding authors

Abstract. The paper presents studies of the properties of thixotropic clay solutions. The mathematical analysis of the processes of creep, relaxation and steady-state flow of the solution on the Shvedov-Kelvin model is carried out. The kinematics of flow of thixotropic clay solution is described.

Keywords: clay solution, thixotropy, Shvedov mode, Bingham mode, pseudolaminar mode, turbulent mode, Shvedov-Bingham model

Introduction

The theory of viscoplastic media currently finds wide application in various scientific fields and is used for the analysis of biological processes, medical issues, in pharmaceutics, development of plastic materials, construction, drilling of oil and gas wells, etc. [1, 2, 3, 4].

For example, in the work of Belarusian scientists S.A. Gavrilenko, R.A. Vasina and S.V. Shilko, defining equations were obtained and identification of biotissue models with viscoplastic properties in the presence of nonlinear velocity sensitivity was performed and rheological constants of blood were determined [5].

In pharmaceutics, the properties of viscoplastic media are used to develop the technology of obtaining various drugs, ointments, etc. [6].

The theory of viscoplastic media has received a significant spread in the use of clay solutions in engineering and construction. During the construction of bearing walls of underground structures and impervious curtains by the "wall-in-soil" method, when drilling oil and gas wells for stability of the walls of trenches and boreholes, the ground is usually developed under clay thixotropic solution. These solutions by rheological properties represent the classical viscoplastic model [7].

Translated with www.DeepL.com/Translator (free version)

The application of clay solution is explained by its important properties: the ability to colmate the walls of the trench (that is, to form a waterproof clay film on them) and keep the particles of the processed ground suspended. At rest, the clay solution is a thick mass-gel, when mechanically exposed to it, the solution is able to change viscosity and liquefy. In this case a viscous liquid is formed that is sol.

The listed properties of viscoplastic media differ significantly from the properties of ordinary viscous liquids, their rheological properties are determined by the complex internal structure, the physical-chemical properties of clay, its concentration in solution.

The clay solution is a two-phase dispersion system in which clay particles are the solid phase, and water is the liquid phase. The surface of solid particles is a phase interface, in the surface layer the dispersion medium has abnormal properties compared to its usual characteristics. Such a layer is called a solvate shell of particles.

Other important properties of clay solutions are: density, viscosity, daily sludge or sedimentation, stability, drainage, thickness of clay crust on the wall of the trench, the ultimate static shear stress, sand content, concentration of hydrogen ions. The density is from 1.08 to 1.5 t/m^3, sedimentation up to 5%, stability - 0.01 t/m^3... 0.02 t/m^3, drainage - 25... 30 cm^3/min, clay crust thickness not more than 4 mm, static shear stress, after a minute holding, not less than 1Pa, sand content not more than 4%, alkali content pH=9,5-10,0. Such viscoplastic properties of clay solution allow it to be used to equip the foundations of temporary bridges and overpasses, which allow to dampen the dynamic load from bridge constructions []

The essence of the processes taking place in viscous-plastic media was revealed by the Soviet and Russian scientists P.M. Ogibalov [9], A.Kh. Mirzadzhanzade [10], V.M. Myasnikov [11] and others.

Clay particles suspended in water make the Brownian motion, force fields are formed around the particles, interacting with each other. With some probability, particles may merge and move together. A similar process can occur with the next particle and so on, resulting in a loose spatial grid that is a coagulation structure. The coagulation structure formed by the adhesion of particles into the chain and disordered spatial grids are the most common kind of dispersed structures. When external mechanical influence on the solution, the force fields of the particles will be distorted. When small intensity of external influence of breaking the connections in the spatial grid, it is possible to transfer particles from one position to another. A relatively small constant load on the medium will cause rearrangement of the framework, the dispersion system comes to a steady state. In case of intense external influence, restructuring of the structural framework cannot ensure the development of a steady-state flow of solution, the loose structural grid is destroyed. The presence of the Brownian motion of clay particles leads to the formation of new connections between them. The dispersion system will be stationary when the number of newly formed connections per unit time is approximately equal to the number of broken connections.

The properties of disperse systems are determined by the relaxation time that is the period during which the connections between the particles of the structural framework are restored and loose spatial structures are again formed in the disperse system. This property of clay and some other solutions is called "thixotropy," which means "variable when touched." Clay solutions have the ability to adapt to external influences. For a qualitative description of the phenomenon of relaxation, the Maxwell equation, from which it follows that the stress state of the system weakens some time later.

Depending on the intensity of external influences on the medium, three types of deformation can develop in the disperse system:

- elastic deformations related to change of interatomic and intermolecular distances;
- elastic deformations when the orientation of the particles in the structural framework changes;
- plastic deformations associated with the movement of coagulation structures.

In addition, it is necessary to take into account the viscous deformation, the influence of which is manifested in the uneven movement of the liquid layers.

In the motion of the viscoplastic solution, the four modes are distinguished:

- the Shvedov mode that is the mode of fluid flow with almost undestroyed structure, occurring with very low rates of movement about several centimeters per second. At the same time, the liquid has the effective Newtonian viscosity η_{ef};
- the Bingham mode that is the liquid flow mode with continuously collapsing structure, occurs at the rate about 1.25 m/s. For this flow mode, the concept of structural viscosity η is introduced;
- pseudolaminar mode that is the liquid flow mode with almost completely destroyed structure; observed at flow rate about 1.5 m/s, the liquid has a dynamic viscosity μ;
- turbulent mode that flows at relatively high rate (more than 2 m/s), while intensive mixing of liquid with fictitious viscosity occurs μ_f.

If a rather intense external influence is applied to the disperse system, then plastic deformations can occur in the system - the movement of individual structures, the pseudolaminar mode of fluid flow can occur and the transition to turbulent, bypassing the Bingham one.

The variable viscosity of the thixotropic solution is associated with a dispersed phase that has some varying structure.

1. Materials and methods

A mathematical analysis of the processes of creeping, relaxation and steady-state flow of solution on the Shvedov-Kelvin generalized mechanical model showed that at very low shear stresses, thixotropic systems have high (about a million pauses) Newtonian viscosity without noticeable destruction of the structure. This viscosity is not detected by conventional rheological methods.

When shear stresses that exceed the limit values significantly, the area of the constant Newtonian viscosity determined in the laminar flow can be distinguished. In a state of viscoplastic flow (the Bingham mode), accompanied by a change and destruction of the structure, the thixotropic solution has structural viscosity. When turbulent flow, the coagulation structures of the clay solution are disturbed, the thixotropic solution has a fictitious viscosity.

The clay thixotropic solution is a two-phase medium in which clay particles are capable to form a complex internal structure. Therefore, a combined rheological model consisting of the simplest models is used as a rheological model of clay solution. Studies have shown that the most accurate rheological properties of clay thixotropic solutions are described by the Shvedov-Bingham model. The strain equation of the viscoplastic medium has the form [9]:

$$\tau = \tau_0 \pm \frac{dV}{dn}, \tag{1}$$

where

- τ – tangent stress of shear;
- τ_0 – extreme stress of shear;
- dV/dn – rate of deformation.

The Shvedov-Bingham model is quite consistent with the physical picture of the motion of the clay solution given above.

The mechanical properties of a solid medium are determined by state equations connecting deformation stress tensors and deformation rate.

If the maximum tangent stress does not exceed the limit stress τ_0, then the viscoplastic liquid behaves as an incompressible elastic body for which the Hooke law is valid:

$$\sigma = E \cdot \varepsilon, \quad \tau = \gamma \cdot G \tag{2}$$

where

- σ – normal stress;
- E – module of elasticity;

- ε – relative deformation;
- γ – angular deformation;
- G – shear module.

If the maximum tangent stress is greater than the viscous flow of the solution.

For the case of the structural mode of fluid flow, it is possible to use the Shvedov-Kelvin model, which gives the following equation for fluid kinematics [10]:

if $\sigma < \sigma_0$:

$$\varepsilon = \frac{\sigma}{E_1} + \frac{\sigma}{E_2}\left(1 - e^{-\frac{t}{t_0}}\right); \tag{3}$$

if $\sigma > \sigma_0$:

$$\varepsilon = \frac{\sigma}{E_1} + \frac{\sigma}{E_2}\left(1 - e^{-\frac{t}{t_0}}\right) + \frac{\sigma - \sigma_0}{\eta} t, \tag{4}$$

where

- σ – stress applied to the system;
- σ_0 - the upper limit of elasticity, or fluidity limit below which the residual deformations are not developed;
- E_1 - initial conditional and instant module of shear;
- E_2 - elasticity module;
- t - process time;
- t_0 - relaxation time.

For viscous flow of viscous-plastic liquid the following equation of state in tensor form [10] is obtained:

$$\sigma_{ij} = \left(\eta + \frac{\tau_0}{v}\right) e_{ij} \tag{5}$$

where

- v – shear rate;
- e_{ij} – deformation strain rate.

For all modes of flow of the clay thixotropic solution, the equation of continuity of the medium will be true:

$$div\left(\rho_c \vec{V}\right) + \frac{d\rho_c}{dt} = 0, \tag{6}$$

where ρ_c – the density of the solution.

For the viscous flow of thixotropic solution (the Bingham and pseudolaminar mode), the differential equations of motion of continuous medium in the Cauchy form will be valid:

$$\rho_c \frac{d\vec{V}}{dt} = \vec{K} + \vec{P}, \tag{7}$$

where

- ρ_c – the density of the liquid;
- dV/dt – is the substantive derivative of the rate of the moving element of the medium;
- $\vec{P}$ – the surface force;
- $\vec{K}$ – the mass force.

For the pseudolaminar mode of flow of the clay solution, the Navier-Stokes equation can be used, provided that the viscosity can be taken as constant:

$$\begin{cases} X - \dfrac{1}{x}\dfrac{dP}{dx} = \dfrac{du_x}{dt} + \nu_\Delta u_x; \\ Y - \dfrac{1}{y}\dfrac{dP}{dy} = \dfrac{du_y}{dt} + \nu_\Delta u_y; \\ Z - \dfrac{1}{z}\dfrac{dP}{dz} = \dfrac{du_z}{dt} + \nu_\Delta u_z, \end{cases} \quad (8)$$

where

- ν – kinematic viscosity;
- u – rate of the fluid

Genki and Ilyushin generalized the Shvedov-Bingham hypothesis about the course of viscoplastic media in the form of differential equations [11]:

$$\frac{d\vec{V}}{dt} = \vec{K} - \frac{1}{\rho_c} gradP. \quad (9)$$

For vortex movements of the viscoplastic medium, the Helmholtz equations are generalized, which have the form [10]:

$$\frac{d\Omega}{dt}(\vec{\Omega}V)\vec{V} + \frac{1}{\rho_c}\left(\eta + \frac{\tau}{\eta_1}\right)\nabla^2\vec{\Omega} + \frac{\tau_0}{\rho_c} rot\Omega \cdot grad\frac{1}{h_1} + \frac{2\tau_0}{\rho_c} gradh_1 \cdot grad\frac{T}{h_1^2}, \quad (10)$$

where $\vec{\Omega} = rot\vec{\nabla}$.

2. Discussion and results

When determining the numerical value of the friction force when the body moves in solution, it is necessary to know the value of the tangent stress τ, which for each flow mode has a certain value.

The Shvedov-Bingam formula is applicable for determining the Bingam mode of solution movement.

For the pseudolaminar mode of solution flow, the stress of friction forces is expressed by the dependence:

$$\tau = \pm\mu\frac{dV}{dh}. \quad (11)$$

The signs "plus" or "minus" are accepted depending on the sign of the gradient of the flow rate of the solution, taking into account the requirement that the stress of the friction forces should be positive.

At turbulent mode of clay solution flow in order to obtain full stress of friction forces it is necessary to add additional voltage from pulsation to the main viscous friction by Newton [11]:

$$\tau = \mu\frac{dV}{dh} + \rho_c l^2\left(\frac{dV}{dh}\right)^2, \quad (12)$$

where l – the average value of the mixing path.

Equation (1) is common for determining the stress of friction forces in the solution of laminar and turbulent flows. In laminar flow, the effect of the flow rate is negligible and the first term of equation (12) prevails for such flow.

In the turbulent flow with a great value of Reynolds number, the influence of the viscosity of the solution, on the contrary, is negligible and here the influence of the second term of the equation is significant.

An important point is the determination of the boundaries of the flow core during the movement of various bodies in a clay solution. So, when the plate moves in solution, the sizes of the flow core can be obtained from the equation:

$$V = \frac{\Delta P}{4l}(H_m - \delta_T) - \frac{\tau_0}{\eta}(H_m - \delta_T), \quad (13)$$

where

- ΔP – the pressure drop in the area under consideration;
- l – the length of the section;
- H_m – the maximum distance from the plate in which the movement is carried out;

- δ_T – the thickness of the boundary layer.

The radius of the viscoplastic flow zone when the smooth cylinder rotates depends on its angular velocity:

$$\left(\frac{r_T}{r}\right)^2 - \ln\left(\frac{r_T}{r}\right)^2 = 1 + \frac{2\mu\omega}{\tau_0}, \tag{14}$$

where

- r_T – radius of spreading of the viscoplastic flow zone;
- r – radius vector of some point of fluid;
- ω – angular rate of rotation of the cylinder.

Conclusions

The given equations of motion and state of the viscoplastic medium are very complex. Therefore, in practice, the problems of the course of such media and the movement of bodies in rheological media are solved by approximate methods that allow you to get a fairly complete picture of the flow and explain the experimental results.

At present, such problems have been solved for the cases of viscoplastic fluid motion in pipes, rotation of a long drill rod in the mud. Due to the differences in the operation of earthmoving machines, it is necessary to carry out investigations to establish the loading process arising from the movement of the working body in the clay solution.

References

[1] Lishchuk V.A. Mathematical theory of blood circulation. - M.: Meditsina, 2011. - 256 p.
[2] Stielman M.I. Biomedical polymers. – M.: ICC "Akademkniga", 2006. – 400 p.
[3] Bortnikov, V.G. Theoretical bases and technology of plastic mass processing. - M.: Infra-M, 2017. – 220 p.
[4] Kadyrova I.A., Mindubaeva F.A., Grjibovski A.M. Prediction of outcomes after stroke: a systematic review //Ekologiya cheloveka (Human Ecology), N. 10, 2015. - P. 55 - 64.
[5] Gavrilenko S.A., Vasin R.A., Shilko S.V. Method of current description and determination of rheological constants of viscoplastic biomaterials //Russian Journal of Biomechanics, № 3, Volume 6, 2002. – P. 92 - 99.
[6] Bykov V.A. Pharmaceutical technology. - M.: GEOTAR-Media, 2009. – 304 p.
[7] Kadyrov A.S., Amangeldiev N.E. New specifications of the theory of ground cutting //Periodico Tche Quimica, Volume 16, Issue 31, 2019. - P. 922 – 936.
[8] Kadyrov A., Ganyukov A., Imanov M., Balabekova K. Calculation of constructive elements of mobile overpass. / Current Science Journal, Volume 116, №9, 2019. – P. 1544 - 1550.
[9] Ogibalov P. M., Mirzadzhanzade A. Kh. Non-stationary movements of viscous-plastic media. - M.: Publishing House of the Moscow university, 1970. – 415 p.
[10] Mirzadzhanzade A.Kh. Issues of hydrodynamics of viscoplastic and viscous liquids in application to oil production. - Baku: Azerneftestroy, 2005. – 409 p.
[11] Myasnikov V.P. Mechanics of hard-plastic media. - M.: Nauka, 2001. – 310 p.

Information of the authors

Kadyrov Adil Suratovich, doctor of technical sciences, professor of the department "Transport Engineering and Logistics Systems" of Abylkas Saginov Karaganda Technical University
E-msil: adil.suratovich@gmail.com

Ganyukov Alexander Anatolievich, PhD, acting assistant professor of the department of "Mechanics" of Abylkas Saginov Karaganda Technical University
E-msil: a.ganjukov@kstu.kz

Altynbaev Aset Zhanatovich, doctoral student of the department o"Transport Engineering and Logistics Systems" of Abylkas Saginov Karaganda Technical University
E-msil: altynbayev.aset@gmail.com

DOI 10.52209/2706-977X_2022_2_20 **IRSTI 53.49.15** **UDC 621.793**

Effect of Spherical Microceramics on Hardness and Wear Resistance of Ni-based Thermal Sprayed Coatings

Lebedev A., Juknevičius T., Škamat Je.*
Vilnius Gediminas Technical University, Vilnius, Lithuania

Abstract. In the present study, the spherical alumina microceramics was used to improve tribological properties and wear resistance of nickel-based thermal sprayed coatings. The powder mixtures containing 5, 10 and 20 wt. % of Al_2O_3 spherical alumina having particles size of 0-40 μm were prepared. The coatings of ~0.9–1.1 mm thickness were formed by two-step spray and fuse process. As a reference, the nickel-based coatings without ceramics addition and nickel-based coatings containing 10 wt. % of Al_2O_3 with angular particles shape was used. The microstructural analysis by scanning electron microscopy showed that after spraying only a part of spherical particles retains their initial spherical shape. The majority of ceramic microspheres melt and form semi-spherical shells surrounding nickel particles and splats. With the addition of 10 wt. % Al_2O_3, the hardness was increased by ~55 %, the mass loss was reduced two times and the friction coefficient diminished by ~35 %. With the increase of ceramics amount up to 20 wt. % Al_2O_3, the worsening of properties was observed, what is related with the local aggregations of ceramic particles in the metal matrix and poor bonds between them.

Keywords: metal matrix composite coatings, nickel-based coatings, aluminium oxide, SEM, tribology, wear.

Introduction

The development of protective coatings technologies undoubtedly is one of the underlying areas of materials engineering. The formation of coatings by thermal spraying process is based on the melting/heating and further deposition of solid materials on the preliminarily prepared surface in a form of dispersed jet. A wide range of used materials enables application of such technologies in the various industrial sectors. There are three main groups of materials used for coatings deposition by thermal spraying – metals alloys, ceramics and composite materials. The present study is focused on the application of aluminium oxide (or alumina) as a valuable component for metal matrix composite (MMC) coatings. Alumina has high melting point (~2 072 °C), hardness (15–19 GPa or 9 on the Mohs scale), compressive strength (2–4 GPa), abrasion resistance and chemical stability along with low density (3.95 g/cm^3) and thermal conductivity (20–30 W/mK). Nowadays, aluminum oxide, among all ceramic material, is one of the most extensively used for deposition of ceramic coating by thermal spray [1]. As shown in a number of publications [1-4], thermally sprayed alumina coatings – single [1, 2, 3] and in combination with other ceramics [4] – possess high hardness (up to 1000 HV0.2). The main problems observed in thermally sprayed ceramics coatings are high porosity, low cohesion of lamellas and coating cracking due to brittleness [3]. In composite MMC coatings, plastic matrix of metal alloy enables to eliminate the problems of porosity, low adhesion and cracking, while ceramics particles incorporated in a metal matrix provide high hardness and wear resistance. However, alumina has not yet been widely used in MMC. Typically, tungsten carbides, chromium carbides, titanium carbide and their combinations are used in MMC [5–13]. In the present study, the spherical microceramics was used. This material has not been yet used for the production of protective coatings. One of the benefits of the particles with spherical shape is its very good fluidity that might contribute to the improvement of powder mixture supply during spraying process. Spherical shape of the particles might have certain effects on the tribological properties of the coatings as well.

1. Experimental details

For the deposition of experimental coatings nickel-based alloy powder (-125/+36 μm) were used having chemical composition in wt. % as follows: ~7.5 % Cr, ~2.5 % Fee, ~0.25 % C, ~1.7 % B, ~3.5 % Si, Ni – balance. As a hardening phase, spherical Al_2O_3 microceramics with particles size 0–40 μm. For the deposition of coatings, three powder mixtures were prepared adding 5, 10 and 20 wt. % of micro-spherical alumina powder to the nickel-based powder. 100 wt. % nickel-based powder was used as a control composition. Moreover, the mixture containing 10 wt. % of alumina with angular particles (3.9–31 μm) was prepared as well for the comparison. Two-step process including oxy-fuel flame spray of the powder mixtures followed by re-fusing of deposited layers in the electric furnace was used to form the coatings. Rototec 80 (Castolin Eutectic) spraying equipment and manipulator Motoman 100 were used for the spraying of powder mixtures. The parameters of spraying process were as follows: neutral flame; 230–250 °C substrate pre-heating temperature; 170 mm spraying distance; 250 mm/s spraying speed; 5 mm step between adjacent passes; 8 spraying layers. The average thickness of the deposited layer was 0.9–1.1 mm. Before spraying, the substrate (steel S235J0, 120×40×8 mm) surface was chemically degreased, grit-blasted, washed with isopropyl alcohol and dried with hot air stream. The re-fusing of deposits in furnace was performed at 1100±10 °C temperature for 5 min.

The microstructural analysis was performed on polished cross-sections of the samples using JEOL JSM-7600F scanning electron microscope at 10 kV accelerating voltage. Microhardness measurements were carried out by Knoop method using Zwick Roell ZHμ tester with a 1 kg load and 10 sec indentation duration. The tribological study was performed by “Ball-on-disc” friction scheme using Microtest tribometer under the following conditions of the experiment:

sliding distance – 500 m, sliding speed – 450 rpm, radius of the trajectory – 2.5 mm, load – 15 N, temperature of the test – 23 °C. The indenter was tempered stainless steel AISI52100 ball of 6 mm diameter.

2. Discussion and results

The microstructural analysis showed that two-step spray-fuse process under indicated parameters enabled to form the uniform low-porous coating (Fig. a). The interface between the coating and substrate uniform, without any gaps and having good physical contact, what provided conditions for chemical interaction and metallurgical bond. Low-porous coatings with strong metallurgical bond were obtained with powder mixtures containing 5 and 10 wt. % of ceramics as well (Fig. 1b-d). Only a part of the spherical particles retained their initial spherical shape. The most of the particles were melted or heated to a temperature sufficient to provide significant plastic deformation of ceramic particles when they collide with the substrate or already deposited particles.

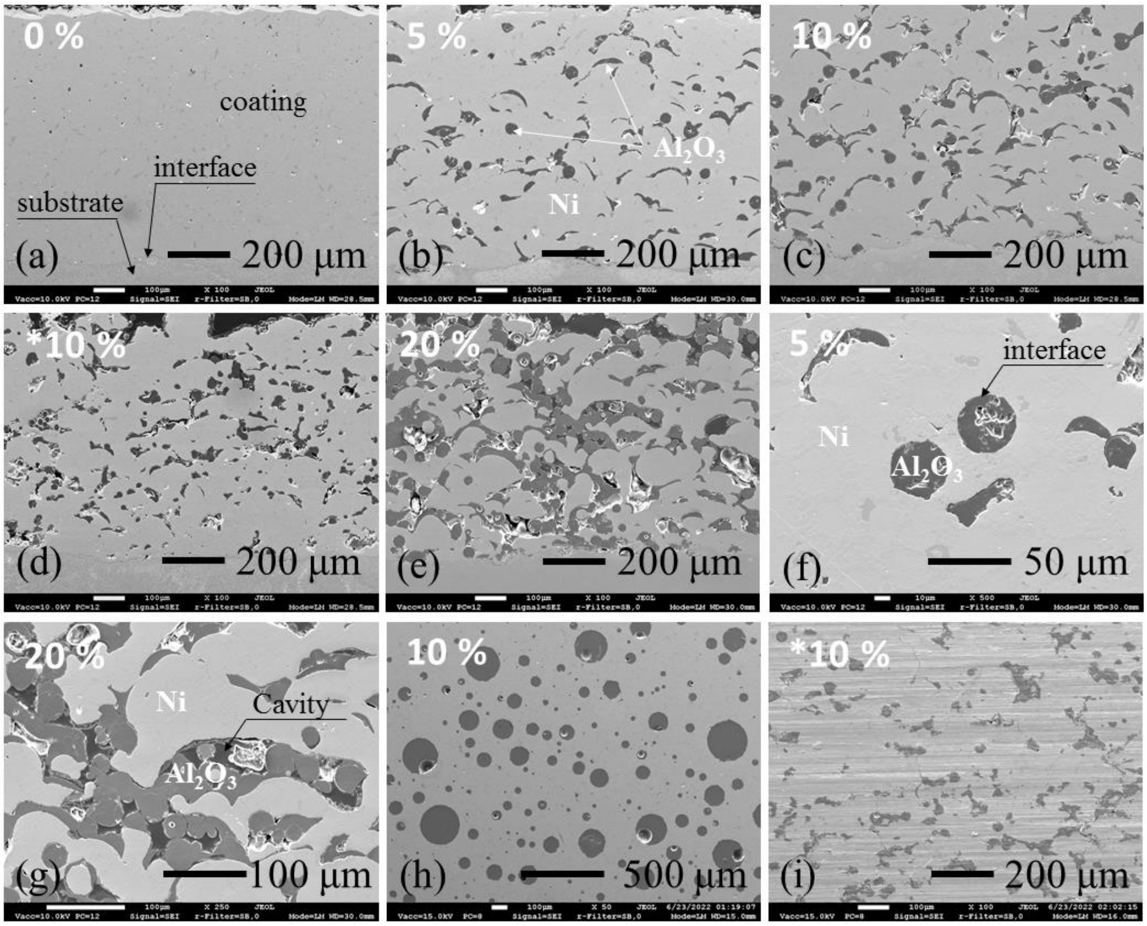

Fig. 1. – The cross-sectional (a-g) and surface (h and i) microstructure of the obtained coatings containing 0 wt. % Al_2O_3 (a), 5 wt. % Al_2O_3 (b), 10 wt. % Al_2O_3 (c, d, h, i) and 20 % Al_2O_3 (e) percent of Al_2O_3; * - ceramics of angular shape; Ni – nickel-based alloy matrix

The melted spherical ceramic particles formed semi-spherical shells surrounding nickel particles and splats. In case of angular alumina particles, the morphology of ceramics inclusions did not differed significantly from that in case of spherical. However, they looked to be finer (Fig. 1d). When ceramics amount was increased to 20 wt. %, the aggregations of ceramic particles were observed, within which the gaps and lack of cohesion between particles can be seen. Nickel-based particles did not form continuous metallic matrix – crystallization of separated micro-volumes of the nickel alloy was observed (Fig. 1e). It can be seen that at lower amount of ceramics (5 % or 10 %), the metal matrix surrounds each inclusion (Fig. 1f), while at higher ceramics concentration, there are a lot of cavities in the coating and ceramic inclusions are poorly incorporated in the matrix (Fig. 1g). The morphology of spherical and angular ceramic micro-inclusions observed from the coatings top was different (Fig. 1h and 1i). The spherical particles have formed round-shaped splats (Fig. 1h) while the shape of splats formed by angular-shaped particles was also angular (Fig. 1i).

The hardness of reference nickel-based coating was ~220 HK0.1 (Fig. 2a). With the addition of alumina, the hardness of the coatings expectably increased and was ~275 HK1.0 at 5 wt. % Al_2O_3 and ~330-340 HK1.0 at 10 wt. % Al_2O_3. It may be noted also that hardness difference of the coatings with spherical and angular microceramics was insignificant. However, when alumina amount was increased up to 20 wt. %, the hardness was reduced, what may be associated with poor cohesion between splats. The mass loss of the coatings during dry sliding wear was reduced with the addition of alumina – by ~9.3% at 5 wt. % Al_2O_3, by two times at 10 wt. % Al_2O_3, and by ~2.6 times at 20 wt. %

Al_2O_3. Despite the hardness of the coating containing 20 wt. % Al_2O_3 showed the decrease compared with the coatings containing 10 wt. % Al_2O_3, the wear resistance was improved, though not so significantly. This may be because the results of hardness (obtained on the cross-sections) were largely dependent on the cohesive strength of the coatings, while for wear resistance the capacity of alumina particles to withstand the compression was the dominant factor.

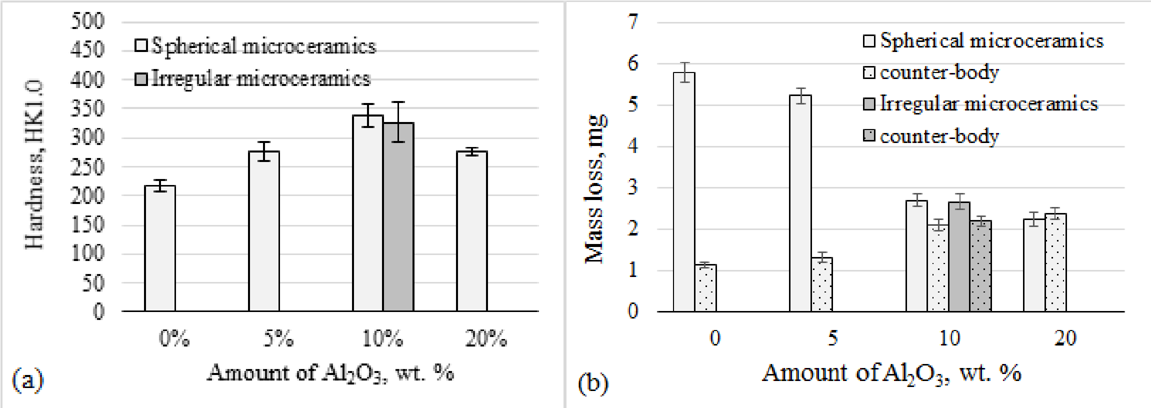

Fig. 2. – Hardness (a) and wear mass loss (b) of the coatings containing different amount of microceramics

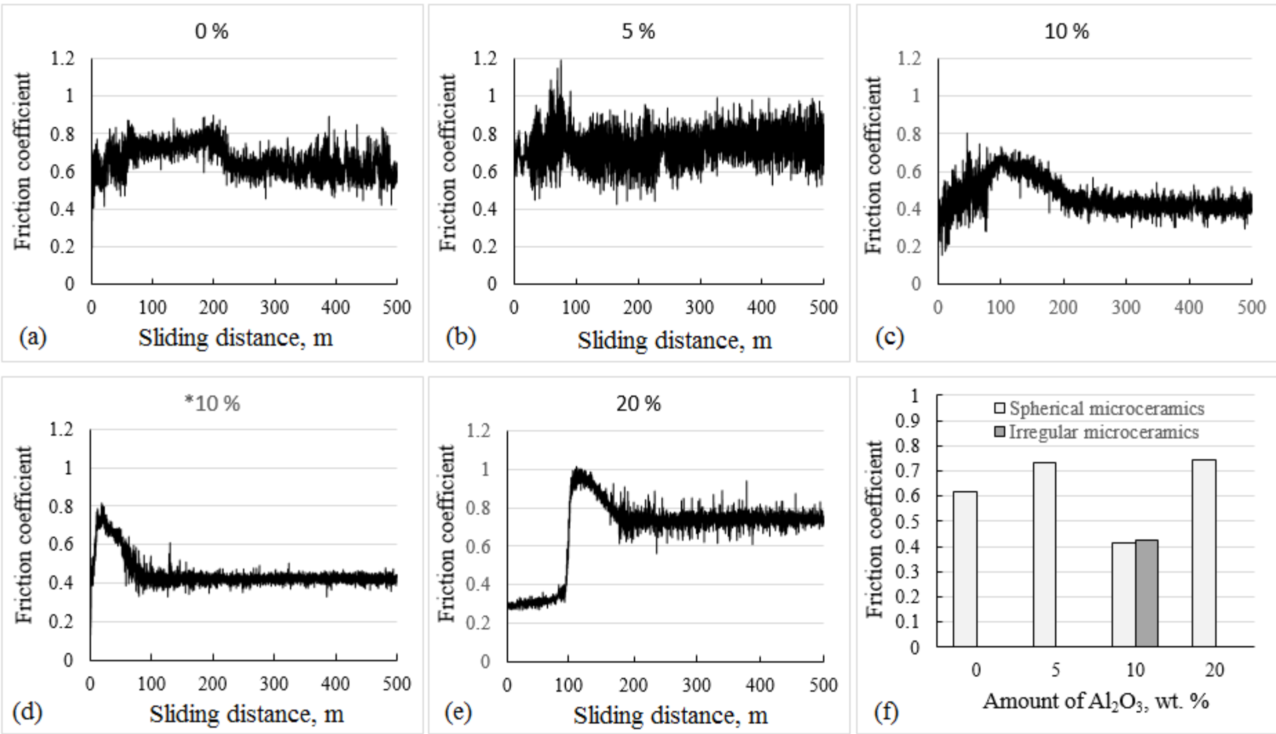

Fig. 3. – Curves of friction coefficient (a-e) and average values of friction coefficient at steady stage (f) for the coatings containing different amounts of alumina

The tribological tests showed that the friction coefficient of the coatings might be visibly reduced with the application of alumina in MMC, what is related with good tribological properties of alumina in general. At the low amount of microceramics (5 wt. %) in the metal matrix, no improvement was observed. However, friction coefficient was visibly reduced when 10 wt. % of alumina was applied. While further increase of microceramics amount in coatings led to the increase in friction coefficient, what may be associated with poor bonds between ceramic particles in the places of their aggregation, resulting in their free falling away and getting between sliding surfaces.

The microscopical analysis of wear traces showed that at the applied load of 15 N the adhesive wear mechanism prevails for both metal coating without alumina addition and MMC coatings containing ceramics (Fig. 4). For metal coating, the presence of signs of plastic deformation was observed as well (Fig. 4a). In MMC coatings, alumina particles act as a support that prevents plastic deformation of the coating surface and displacement of metal layers under load (Fig. 4c). The crumbling out of the alumina particles was not observed.

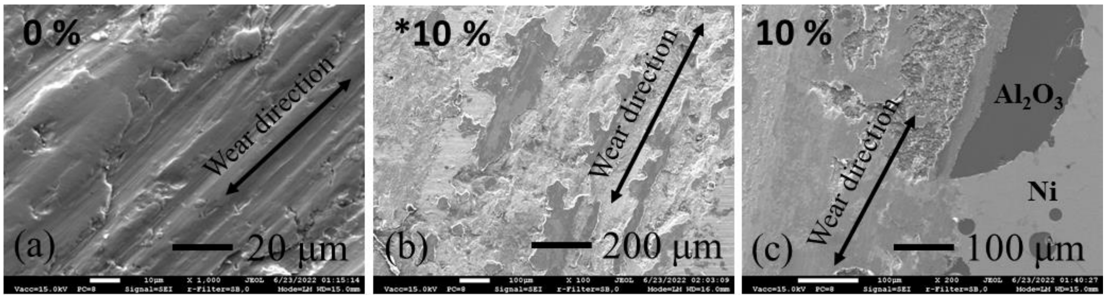

Fig. 4. – Wear tracks of nickel-based coating (a) and coatings containing 10 wt. % of angular (b) and spherical (c) Al_2O_3

Conclusions

Based on the results of the performed experiments one may summarize that application of spherical alumina ceramics in metal matrix composite coatings enables to improve their wear resistance and tribological behavior. Addition of 10 wt. % Al_2O_3 to nickel-based alloy provided reduction of mass loss of the coating during dry sliding wear by ~2 times and friction coefficient by ~35 %. Addition of 5 wt. % Al_2O_3 was too small to obtain any improvement of properties. At 20 wt. % of Al_2O_3, the friction coefficient was increased while the improvement of wear resistance was insignificant, as compared with that at 10 wt. % of Al_2O_3. The main factor, which predetermined worsening of coatings performance at higher alumina amount, was the aggregations of ceramic particles, where cohesion between them was poor. The improvement of tribological properties and wear resistance is obtainable, when proper metal matrix to ceramic particle volume ratio is applied, providing good incorporation of ceramic particles in the metal matrix and avoiding an aggregation of the ceramic particles.

References

[1] Michalak M., Latka L., Sokolowski P., Toma F.-L., Myalska H., Denoirjean A., Ageorges H. Microstructural, mechanical and tribological properties of finely grained Al_2O_3 coatings obtained by SPS and S-HVOF methods. //Surface and Coatings Technology, Vol. 404, 2020. 126463.

[2] Goel S., Björklund S., Curry N., Wiklund U., Joshi SV. Axial suspension plasma spraying of Al_2O_3 coatings for superior tribological properties //Surface and Coatings Technology, Vol. 315, 2017. – P. 80 - 87.

[3] Bolelli G., Rauch J., Cannillo V., Killinger A., Lusvarghi L., Gadow R. Microstructural and tribological investigation of high-velocity suspension flame sprayed (HVSFS) Al_2O_3 coatings //Journal of Thermal Spray Technology, Vol. 18, 2008. – P. 35.

[4] Liu Y., Fischer T. E., Dent A. Comparison of HVOF and plasma-sprayed alumina/titania coatings—microstructure, mechanical properties and abrasion behavior //Surface and Coatings Technology, Vol. 167, Iss. 1, 2003. – P. 68 - 76.

[5] Aguero A., Camon F., Garcıa de Blas J., Hoyo J.C, Muelas R., Santaballa A., Ulargui S., Valles P. HVOF-deposited WCCoCr as replacement for hard Cr in landing gear actuators. //Journal of Thermal Spray Technology, Vol. 20, Iss. 6, 2011. – p. 1292-1309.

[6] Guilemany J.M., Espallargas N., Suegama P.H., Benedetti A.V., Fernández J. High-Velocity oxyfuel Cr_3C_2-NiCr replacing hard chromium coatings. //Journal of Thermal Spray Technology, Vol. 14, Iss. 3, 2005. – P. 335 - 341.

[7] Song B., Murray J.W., Wellman R.G., Pala Z., Hussain T. Dry sliding wear behaviour of HVOF thermal sprayed WC-Co-Cr and WC-CrxCy-Ni coatings. //Wear, Vol. 442 – 443, 2020. – P. 203114.

[8] Bhosale D.G., Rathod W.S., Rukhande S.W. Effect of counter faces on sliding wear behavior of WC-Cr_3C_2-Ni composite coating deposited by high velocity oxy fuel. //Materials Today: Proceedings, 2020. https://doi.org/10.1016/j.matpr.2020.08.466

[9] Jagadeeswar A.S., Kumar S., Venkataraman B., Babu P.S., Jyothirmayi A. Effect of thermal energy on the deposition behaviour, wear and corrosion resistance of cold sprayed Ni-WC cermet coatings. //Surface and Coatings Technology, Vol. 399, 2020. 126138.

[10] Guo H., Li B., Lu C., Zhou Q., Jia J. Effect of WCeCo content on the microstructure and properties of NiCrBSi composite coatings fabricated by supersonic plasma spraying. //Journal of Alloys and Compounds, Vol. 789, 2019. – P. 966 - 975.

[11] Zhang M., Li M., Chi J., Wang S., Yang S., Yang J., Wei Y. Effect of Ti on microstructure characteristics, carbide precipitation mechanism and tribological behavior of different WC types reinforced Ni-based gradient coating //Surface and Coatings Technology, Vol. 374, 2019. – P. 645 - 655.

[12] Smith G.M., Gildersleeve E.J., Luo X.-T., Luzin V., Sampath S. On the surface and system performance of thermally sprayed carbide coatings produced under controlled residual stresses //Surface and Coatings Technology, Vol. 387, 2020. 125536.

[13] Bolelli G., Colella A., Lusvarghi L., Morelli S., Puddu P., Righetti E., Sassatelli P., Testa V. TiC–NiCr thermal spray coatings as an alternative to WC-CoCr and Cr_3C_2–NiCr //Wear, Vol. 450-451, 2020. 203273.

Information of the authors

Lebedev Aleksandr, master of engineering sciences, PhD student of the department "Mechanical and Materials Engineering" of Vilnius Gediminas Technical University.
E-mail: aleksandr.lebedev@vilniustech.lt

Juknevičius Tautvydas, bachelor of engineering sciences in manufacturing engineering, master's degree student of the department "Mechanical and Materials Engineering" of Vilnius Gediminas Technical University.
E-mail: tautvydas.juknevicius@stud.vilniustech.lt

Škamat Jelena, doctor of technology sciences, senior research fellow of the Laboratory of Composite Materials of Vilnius Gediminas Technical University.
E-mail: elena.skamat@vilniustech.lt

DOI 10.52209/2706-977X_2022_2_24 **IRSTI 53.33.33** **UDC 622.28**

Determination of Loads on the Elements of Mechanized Supports

Zhetessov S.S., Abdugaliyeva G.B.,Okimbayeva A.E., Nikonova T.Yu.*
Abylkas Saginov Karaganda Technical University, Karaganda, Kazakhstan
*corresponding author

Abstract. An experimental study of the support for the mechanized repayment of the under-roofing coal layer is given. Determining the parameters of the new cleaning space. The results of the research are shown that when working out layers K_{12} and D_6, the pitch of the collapse of the rocks of the main roof ranges from 15 to 20 m. Laboratory studies of measurements of loads on the upper floor of the support were carried out: during the movement of the support, during the excavation and after the excavation of coal.

Keywords: equivalent material, heading-and-bench, overhand shape of face, loosening, collapse, extended and active unloading zone, supporting, rock pressure, the concentration of maximum stresses

Introduction

Based on the operational and technical requirements, modern mechanized supports should provide reliable protection of the working space of the treatment face from the penetration of lateral rocks into it and safe working conditions in lavas, roof management, methods of complete collapse or smooth lowering and movement following the movement of the treatment face. The support should be controlled in the plane of the formation and in a plane perpendicular to its occurrence and providing directional movement of its section following the movement of the face [1 - 4].

Resistivity of supporting type supports (average) q is taken depending on the thickness of the layers within: m $\ll$1 m, q$\gg$200 kN/m^2; m=1-2 m, q$\gg$300 kN/m^2; m>2 m, q$\gg$400 kN/m^2. The resistivity of the supporting parts (average) of the protective-supporting type supports in relation to conditions with easily collapsible roofs, weak coals and shallow bedding from the surface is 200 kN/m^2 [5].

The height and extensibility of the support struts must correspond to the reservoir capacity and are accepted depending on the actual values of power fluctuations within the excavation column. In addition, when choosing the minimum and maximum size of the support in height, the amount of lowering of the roof and the margin of compliance of the support for unloading are taken into account [6, 7].

The dimensions (width and height) of the free passage of people between the protruding parts of the equipment should be at least 0.7 × 1.5 m.

The support should pick up the roof when coal is excavated, preventing prolonged exposures of the roof strip along the face of the entire lava with a width of more than 0.3 m (with an exposure of more than 1 hour) and short-term exposures (less than 10 minutes) for shallow layers from 0.8 to 1 m of sections more than 8 m^2 and for layers 1-2 m of roof sections more than 10 m^2 [5, 6].

The forces transmitted by the front ceiling consoles to the roof should be at least 15-20 kN. When the length of the overlap console is more than 1 m, its end is active, i.e. having freedom of deviation relative to the rest of the overlap up and down at an angle of at least ± 10 °.

The distance from the face to the front row of the support posts does not exceed 1.5 m, and the initial spacer is 40-50% of the working resistance. The movement of the supporting parts of the support, especially with a weakly resistant roof, must be carried out with residual support of up to 20 kN /m^2 [7].

1. Methodology

It is established that the pressure on the supporting parts of the supports is distributed unevenly and increases from the face to the blockage according to a law close to trapezoidal, with a base ratio of up to 1: 10 or more.

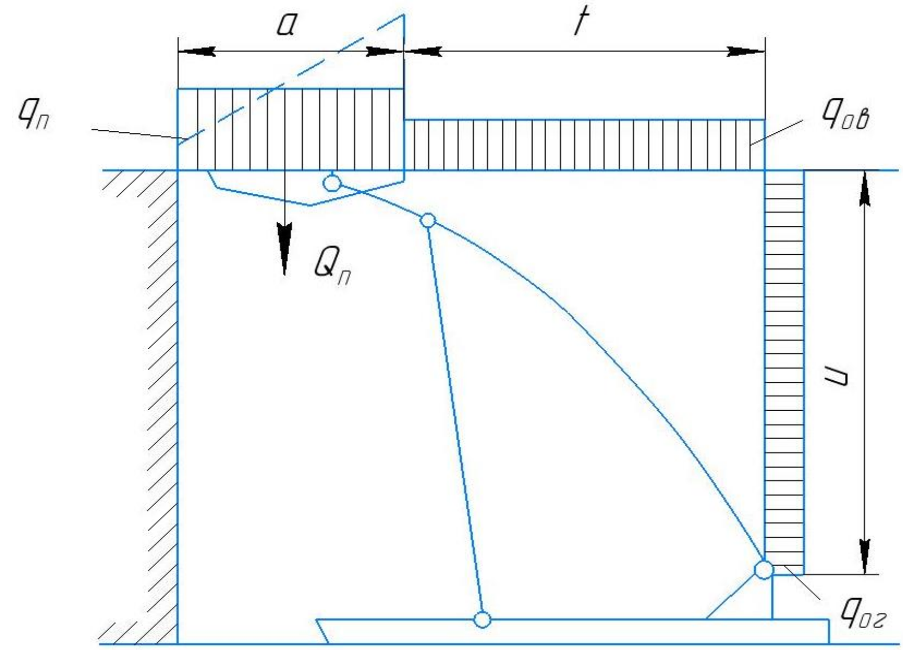

Fig. 1. - Loads on the supporting and protective elements of the protective and supporting supports

With single-support supporting parts, rock pressures are conditionally set evenly distributed over the area of the supported roof (Fig. 1), and with two or more supporting ones distributed over the width of the supported strip according to the trapezoidal law (Fig. 2) with bases q = 30 kN/m^2 at the bottom of the face and q= 370 kN/m^2 at the blockage end [7].

The rock pressure on the protective parts is set as a uniformly distributed component vertically q = 150 kN/m^2 and horizontally q = 80 kN/m^2.

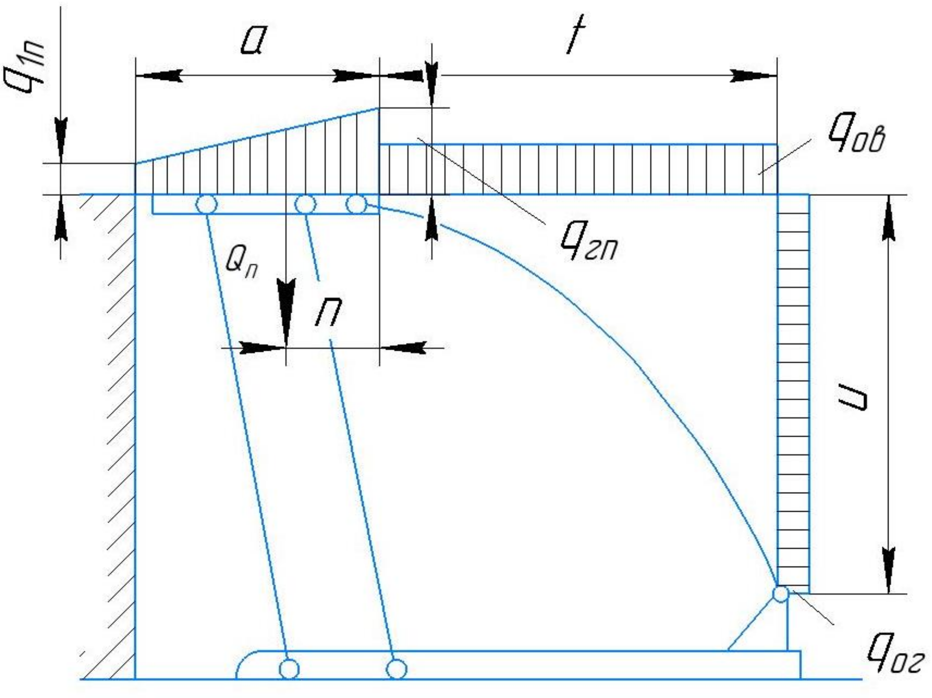

Fig. 2. - Loads on the supporting and protective elements of two or more supporting protective and supporting supports

The total load on the supporting elements will be determined for single-support supports:

$$Q_p = q_{p.avg} a \cdot b, \tag{1}$$

If $Q_{s.pr}$ - the specific resistance of the support (equal to 200 kN/ m^2); a - width of the supported roof strip, m; b - installation step, m.

For multi-support supports:

$$Q_p = \frac{q_{1p} - q_{2p}}{2} ab. \quad (2)$$

The distance of the point of application of force from the rear end of the supporting part is equal to

$$h = \frac{q_{2p} - 2q_{1p}}{3(q_{1p} + q_{2p})} a. \quad (3)$$

The total vertical and horizontal forces on the protective part are determined depending on its configuration. With protective parts outlined in a circle:

$$Q_{o.v} = q_{o.v} \cdot t \cdot b; \quad (4)$$

$$Q_{o.v} = q_{o.v} \cdot U \cdot b, \quad (5)$$

Where t and U are vertical and horizontal projections of the protective part.
The total pressure is equal to:

$$N_o = \sqrt{Q_{o \cdot v}^2 + Q_{o \cdot r}^2} \quad (6)$$

The resulting force passes through the middle of the chord and perpendicular to it (see Fig. 2).
With fencing elements having a complex configuration, the fence is conditionally divided into sections, provided that the ratio of the length of the chord and the height of the segment is at least 20 (Fig. 3).
If the angle of inclination is less than 20°, the load on this section is assumed to be distributed along a trapezoid with bases: $q'_{1o \cdot v}$=370 kN/m^2. $q''_{1o \cdot v}$=200 kN/m^2 [3, 4].
The vertical and horizontal components of the loads acting on the plot with a rectilinear plot are calculated using the formulas:

$$Q_{i\,o.v} = q_{o.v} \cdot t_1 \cdot b; \quad (7)$$

$$Q_{i\,o.v} = q_{o.v} \cdot U_1 \cdot b, \quad (8)$$

Where t_i and U_i - horizontal and vertical projections of the i-th section, m.
The resultant horizontal and vertical components corresponding to uniform pressure plots are defined as follows:

$$N_i = \sqrt{Q_{i\,o \cdot v}^2 + Q_{i\,o \cdot r}^2} \quad (9)$$

For sections with angles < 20 °, the normal forces will be equal to:

$$N_{ir} = Q_{i\,o \cdot v} \cdot \cos \alpha_i; \quad (10)$$

$$N_{iv} = Q_{i\,o \cdot r} \cdot \sin \alpha_i. \quad (11)$$

The resultant of the loads on the protective part is found by constructing a polygon of forces, and the line of its action is by constructing a rope polygon (see Fig. 3).

2. **Determination of the working resistance of hydraulic support posts.**

The working resistance of the support is calculated taking into account the loads from the pressure of the rocks N_p and N_o, the own weight of the support G, the friction and contact forces of the supporting and protective elements with the side rocks, and the forces acting on the protruding elements of the base of the support N [6].

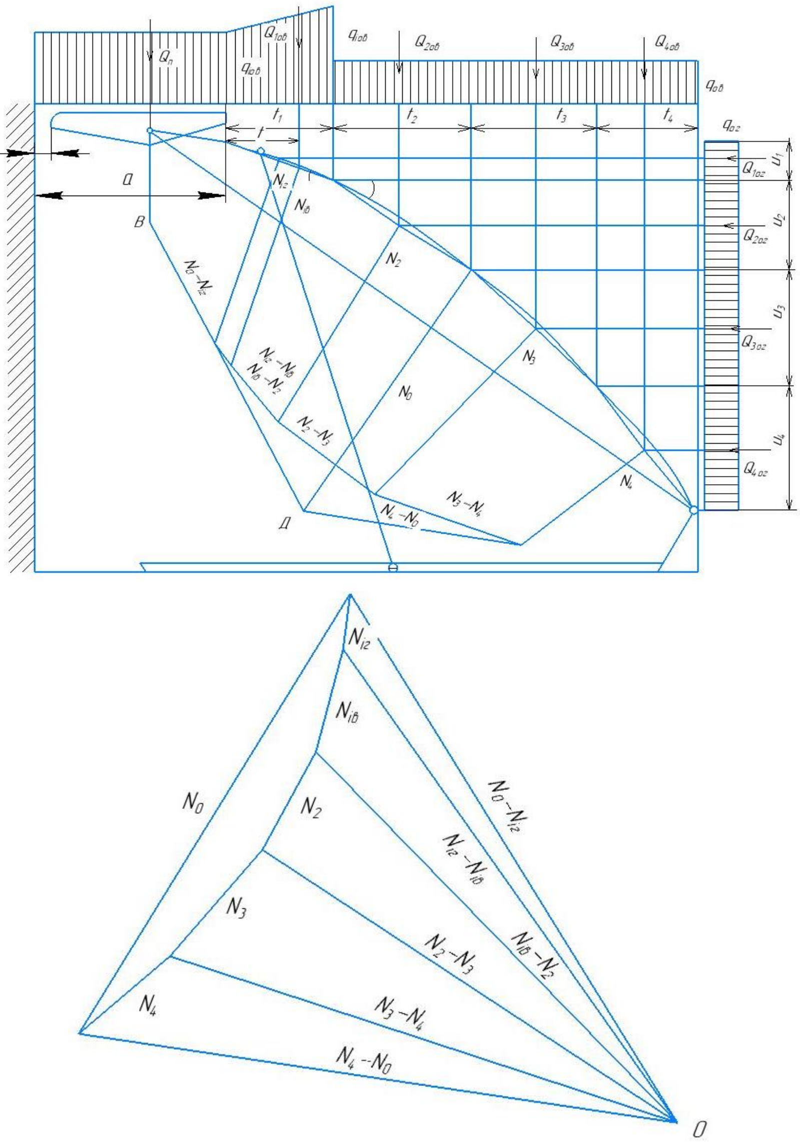

Fig. 3. - Loads on protective elements having a complex configuration

The direction of action of the friction forces is chosen opposite to that in which it is possible to overturn the section due to the absence of friction forces. To do this, a polygon of forces and a rope polygon are constructed, we find the resultant of the forces Np, N, N', G acting on the section, without taking into account the friction forces (Fig. 4).

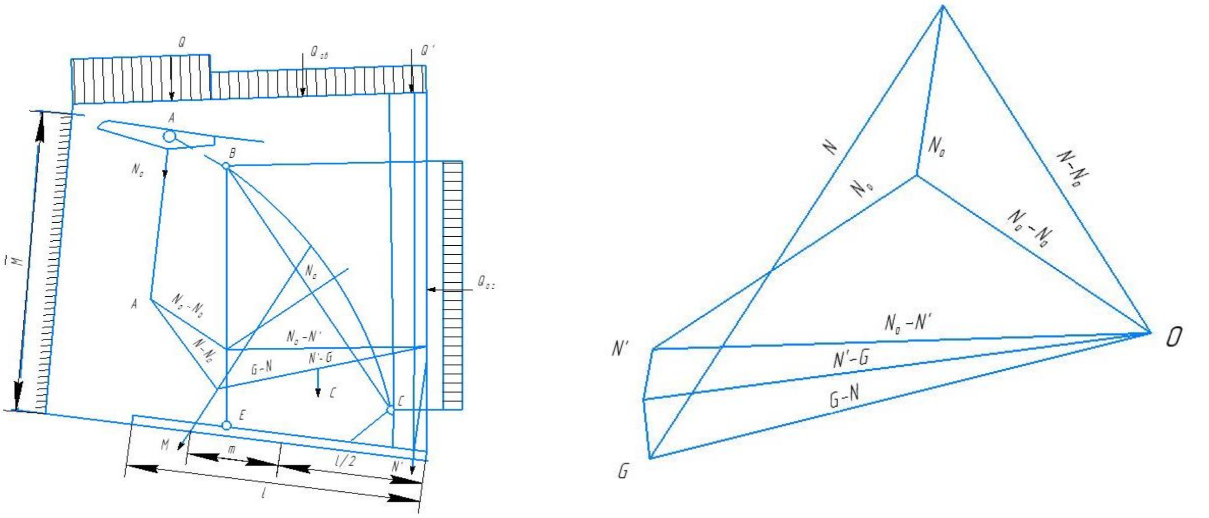

Fig. 4. - Determination of the point M and the intersection of the resultant force with the base of the support

If point M lies to the left of the middle of the reference length of the base (point D), then the section tends to tip over counterclockwise. The direction of the friction forces for this case should be chosen so as to prevent overturning.

The acting friction forces are equal:

$$F = f \cdot N_t. \tag{12}$$

To determine the calculated values of the coefficients of friction at rest, the tipping moment of the active forces $M_{a.k}$ and relative to the middle of the reference length of the base of the friction forces $M_{tr}$is calculated (Fig. 5)

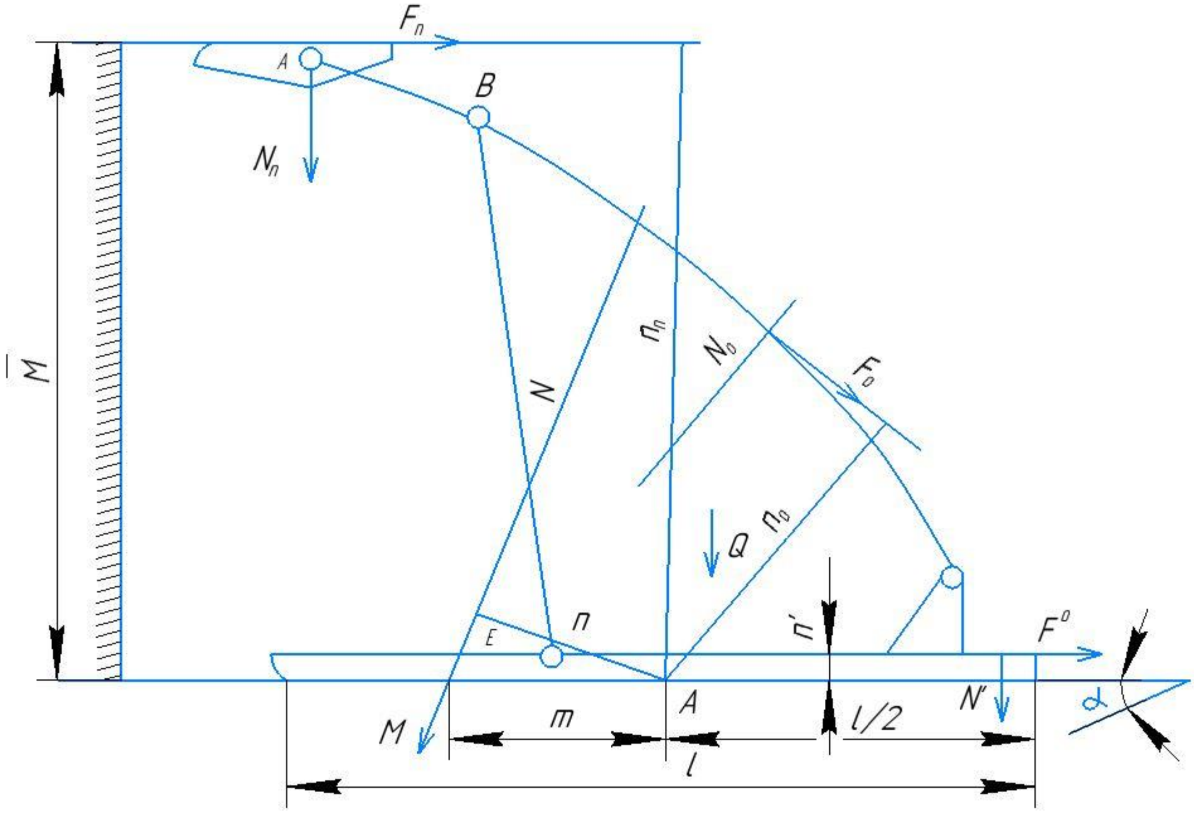

Fig. 5. - Determination of the moment of tipping forces acting on the section

$$\mathrm{M}_{a.k} = N \cdot h; \tag{13}$$

$$\mathrm{M}_{tr} = F_p \cdot h_p + F_0 h_0 + F' \cdot h' \tag{14}$$

or

$$\mathrm{M}_{tr} = f\left(N_p \cdot h_p + N_0 h_0 + N' \cdot h'\right). \tag{15}$$

Equating the right parts (13) and (14), we get:

$$f = \frac{Nh}{N_p h_p + N_0 h_0 + N' h'}. \tag{16}$$

The coefficient of friction of metal on rock (f_0) is assumed to be 0.40. If it turns out that $f < f_0$, then the friction forces are calculated by the coefficient of friction f. When $f > f_0$, the calculation is carried out by f_0=0.40. The support posts perceive the pressure of the lateral rocks acting on the supporting and protective elements, the resultant of which is the geometric sum of the forces P_p and P_o. on the supporting and protective parts of the support. In turn, the forces P_p and P_0 are the resultant of normal forces and friction forces (Fig. 6). The point of intersection of the resultant with the axis of ALL hydrostoy determines the line of action of the reaction in the hinge R_{SH}.

The decomposition of the force R is the reaction of the hydrostocks R_C and R_{SH} of the hinge [9, 10].

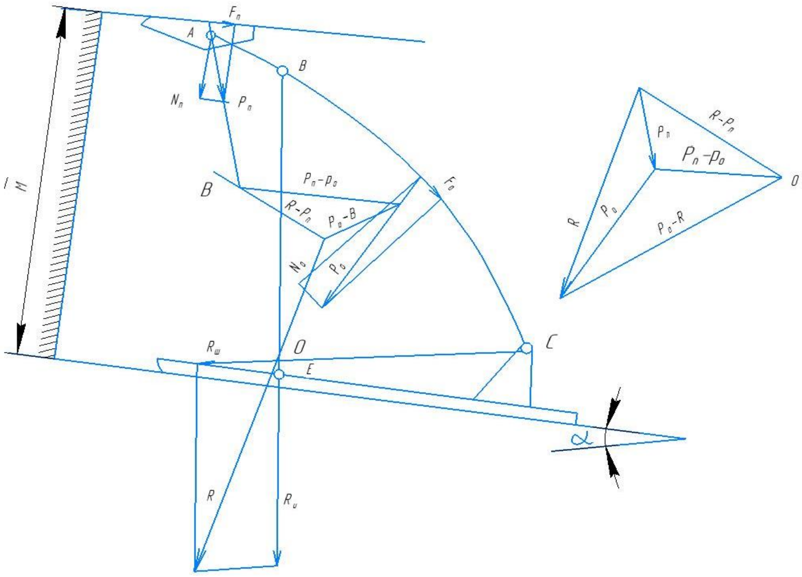

Fig. 6. - Determination of the forces acting on the rack and in the hinge of the rack when the protective part is supported on one hinge

For the supports of the protective-supporting type, when the fence is supported not on one hinge, but on two levers, the equation of moments from the forces R and Rc is drawn up relative to the point O obtained by the intersection of the lines of action of forces C and D (Fig. 7).

From the equation of moments is determined by:

$$R_C = \frac{Rh_1}{h_2}; \tag{17}$$

Next from the polygon of forces are C and D.

3. Determination of the parameters of the power elements of the support section of the protective-supporting type when moving with a residual support

In contrast to the existing protective type supports, the strut of the protective-supporting supports is made by pliable racks. This allows you to adjust the height of the support section depending on the power of the layers being removed.

When working with such fasteners on the lower layers, deformation of the coal bundle is possible. To avoid coal dumping at the bottom of the face during movement and to ensure the stability of the section in the structure, it is necessary to provide a sprung visor [8 ,9].

In order to select the parameters of the power elements of the section of this design, we will consider the process of its movement with the residual strut of the racks.

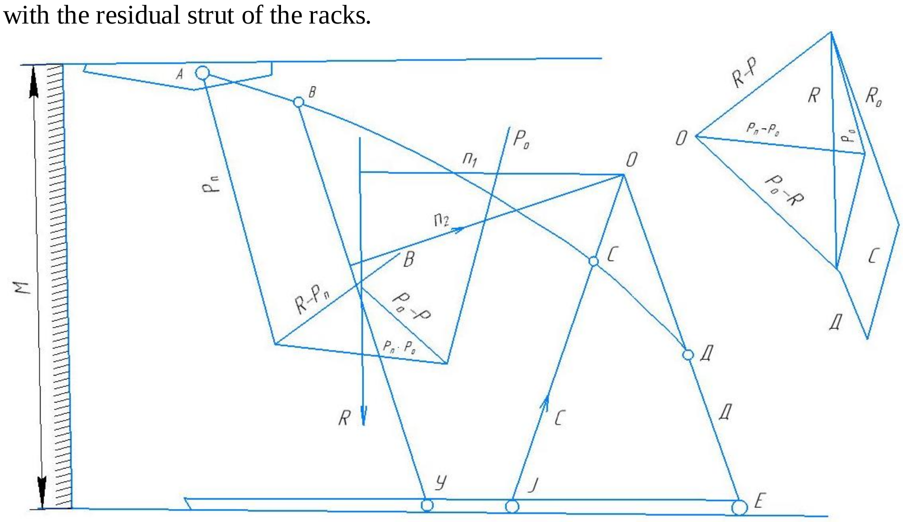

Fig. 7. - Determination of the forces acting on the rack and in the levers when leaning on two levers

The differential equations of motion of the sections (Fig. 8) are as follows:

$$M_{\mathrm{c}}\frac{d^2X_c}{dt^2} = P_A - (T_v + T) - P_c \sin\alpha_1\,; \tag{18}$$

$$M_{\mathrm{c}}\frac{d^2Y_c}{dt^2} = P_c \cos\alpha_1 - N + H_1\,; \tag{19}$$

$$I_c = \frac{d\omega}{dt} = -P_A \cdot d - T_v \cdot a6 + T \cdot b + N \cdot e + H_1 k, \tag{20}$$

where H_1 is the resistance force of the canopies to the roof, kN/m^2:

P_{c} is the weight of the section, kN;

P_A is the movement force, kN; T_v is the friction force of the canopy on the roof, kN;

T is the friction force of the base on the soil, kN;

M_c is the mass of the section, kg; α_1 is the angle of incidence of the formation, deg;

N is the reaction of the soil, kN;

f is the coefficient of friction of steel on coal;

I_c is the moment of inertia of the section relative to the axis passing through the center of gravity and perpendicular to the xoy plane, m;

C is the center of gravity of the section.

We assume that the section moves in a straight line. The axis passes through the center of gravity of the section, therefore, from equation b (19) we have:

$$N = H_1 + P_c \cos\alpha_1 \tag{21}$$

From equation (18) we obtain:

$$\frac{d^2X_c}{dt^2} = \frac{1}{\mathrm{M_c}}[P_A - (T_v + T) - P_c \sin\alpha_1]\,;$$

$$\frac{dX_c}{dt} = \frac{t}{M_c}[P_A + P_c \sin\alpha_1 - (T_v + T)] + C_c;$$

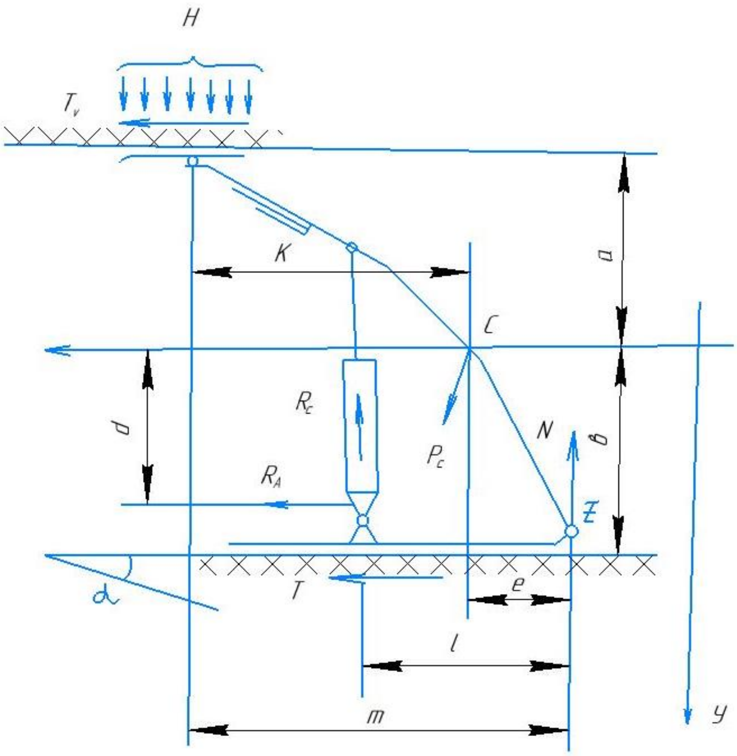

Fig. 8. - Calculation scheme for determining the forces of movement of sections depending on loading

It is known that for t= 0 V_p^c= 0, hence C_1= 0

$$X_c = \frac{t}{2M_c}[P_A + P_c \sin\alpha_1 - (T_v + T)] + C_2;$$

for t=0, X_c=0, so C_2=0. Then:

$$X_c = \frac{t^2}{2M_c}[P_A + P_c \sin\alpha_1 - (T_v + T)]; \tag{22}$$

$$X_c = \frac{gt^2}{2P_c}[P_A - (T + T_v - P_c \sin\alpha_1)].$$

For $\alpha_1 = 0$

$$X_c = \frac{gt^2}{2P_c}[P_A - (T_v + T)];$$

for $\alpha_1 < 0$

$$X_c = \frac{gt^2}{2P_c}[P_A - (T_v + T) + P_c \sin\alpha_1)].$$

From equation (20) we have

$$\frac{d\omega}{dt} = \frac{1}{I_c}(-P_A \cdot d - T_v a + T \cdot b + Ne + H_1 k);$$

$$\omega = \frac{t}{I_c}(Tb + Ne + H_1 k - P_A d - T_v a) + C_3;$$

For t=0 ω_0= 0, hence C_3 - 0.
In addition, ω=0, since the motion is rectilinear.
Finally,

$$Tb + Ne + H_1 k - T_v a = P_A d.$$

From here:

$$P_A = \frac{T \cdot b + N \cdot e + H_1 \cdot k - T_v \cdot a}{d} \tag{23}$$

To establish the place of application of the soil reaction, we make up the equation of moments relative to the point O:

$$\sum M_z = P_c e + H_1(k + e) - T_v(a + d) + T(b - d); \tag{24}$$

and considering that:

$$T_v = H_1 \cdot f; \quad T = (H_1 + P_c)f \tag{25}$$

We have:

$$e = \frac{H_1 \cdot f(a+d) - (H_1 + P_c) \cdot f \cdot (b-d) - H_1 k}{P_c + H_1}$$

Substituting the values of the shoulders and taking f = 0.3, we find H = 147 kN, e =-0.84 m.
Then:

$$P_A = \frac{(H_1 + P_c)fb - (H_1 + P_c \cos\alpha_1)e + H_1 k + Hfa}{d} \tag{26}$$

Conclusions

In conclusion, we would like to note that the movement force P_A increases with an increase in the loading and weight of the section and decreases with an increase in the angle of incidence of the formation α_1. It was found that during the development of layers K12 and D6, the pitch of the collapse of the rocks of the main roof ranges from 15 to 20 m.

References

[1] Abdugalieva G. B. research of indicators and trends of technological machines in the production of gravitational coal: Textbook - Karaganda: Publishing house of KSTU, 2020. – 90 p.
[2] Abdugalieva G. B., Okimbayeva A. E., Kainazarov A. K., Nogaev K. A. basic equipment of the cleaning face: textbook. – Karaganda: KSTU publishing house, 2021. – 80 p.
[3] Zhetessova G.S., Zhetessov S.S., Abdugalieva G.B. The path of development of mining technological machines based on engineering calculations: textbook. - Karaganda: KSTU publishing house, 2014. - 76 p.
[4] Zhetessov S.S., Yurchenko V.V., Abdugalieva G.B. Investigation of technological parameters of a drift conveyor when excavating coal with lowering blocks //Proceedings of the International Conference "Science and education - the leading factor of the strategy "Kazakhstan-2030". - Karaganda: Publishing house of KSTU, 2008. - P. 40 – 41.
[5] Zhetessov S.S., Beisembayev K.M., Abdugalieva G.B. Managing an array of mechanized supports // Proceedings of the International Scientific and Practical Conference, "Science and education - the leading factor of the strategy "Kazakhstan-2030" A.S. Saginovsky readings No. 2. (June 24-26, 2010). Part III - Karaganda: Publishing House of KSTU, 2010. - P. 155 – 157.
[6] Zhetessov S.S., Dzhumagaziev N.B., Abdugalieva G.B. The main directions of improving the technology of cleaning works //Proceedings of the Moscow State Mining University. - M.: Publishing House of Moscow State University, No. 7, 2009. - P. 123 - 125.
[7] Zhetessov S.S., Beisembayev K.M., Abdugalieva G.B. Gravitationalyk komirdi ondirudegi technologiyalyk mashinalardyn korsetkishteri men urdisterin zertteu: Monograph -Karaganda: KSTU Publishing House, 2011. - 108 p.
[8] Tir I.D., Klimov Yu.I. et al. Calculation and selection of equipment of a mechanized complex for mechanization of cleaning operations at coal mines: Textbook -Karaganda: Publishing house of KSTU, 2014. - 106 p.
[9] Zhetessova G. S., Zhetessov S. S., Abdugalieva G. B. The Path of development of mining technological machines based on engineering calculations: textbook-Karaganda: KSTU publishing house, 2014. – 93 p.
[10] Tir I.D., Klimov Yu.I. et al. Modern mining equipment: Part 1. Cutter loader combines: Textbook-Karaganda: Publishing house of KSTU, 2014. – 228 p.

Information of the authors

Zhetessov Santay Suleimenovich., doctor of technical sciences, professor of department "Technological equipment, mechanical engineering and standardization" of Abylkas Saginov Karaganda Technical University
E-mail: zhetesov_s@mail.ru

Abdugaliyeva Gulnur Baimurzaevna, candidate of technical sciences, associate professor of the department "Technological equipment, mechanical engineering and standardization" of Abylkas Saginov Karaganda Technical University
E-mail: gulnura84@mail.ru

Okimbayeva Asel Erkinovna, lecturer of the department "Technological equipment, mechanical engineering and standardization" of Abylkas Saginov Karaganda Technical University
E-mail: erkinovna89@mail.ru

Nikonova Tatyana Yurievna, candidate of technical sciences, acting associate professor of the department "Technological equipment, mechanical engineering and standardization" of Abylkas Saginov Karaganda Technical University
E-mail: nitka82@list.ru

DOI 10.52209/2706-977X_2022_2_33 IRSTI 81.09.01 UDC 378.016:620.22

Methods of Teaching and Control of Knowledge in the Course "Material Science"

Smolkin A.A.*
Moscow State University of Mechanical Engineering (MAMI), Moscow, Russia
*corresponding author

Abstract. Innovative methods for studying rod assemblies and, in particular, sections on the development of the most used iron-carbon alloys are considered in the article. The methodical system of teaching in the course "Materials Science" is described, taking into account didactic principles. The priority methods in teaching the course "Materials Science" are given. The factors that increase the independence of students in the study of the course are indicated. Effective techniques for controlling students' knowledge after studying the course "Materials Science" are given.

Keywords: state diagrams, iron-carbon alloys, liquidus and solidus curves, bank of test tasks, computer testing

Introduction

In recent years, in the conditions of market relations and the need to create new machines and designs in various industries that meet world standards, the list of materials with increased requirements for strength, heat resistance, corrosion resistance and reagent resistance has expanded. During operation, the materials selected by designers and engineers are subjected to various operational loads, therefore, when studying materials science and technology of building materials, it is necessary to disclose in more detail modern, recognized in scientific practice, mechanisms of destruction of materials [1].

The task of materials science is to establish the patterns of the relationship between the structure and properties of materials in order to purposefully influence them during processing into products and operation, as well as to create materials with specified combinations of properties and predict the service life of materials.

The operating conditions of materials have become more stringent due to increased production, pollution and an increase in the aggressiveness of the environment. Active human intervention in natural processes has led to the attention of science to the protection of the environment, the identification of secondary resources. The solution of this "technically neutral" problem by means of materials science has a certain economic and social orientation [2].

Today, the course "Materials Science" with its attribution is provided for the majority of undergraduate and graduate students of engineering and technical specialties, taking into account their professional orientation. The course has certain problems that are a result of the reduction in academic hours for this course and its difficulty for students due to complexity, descriptiveness and verbosity.

1. The content of the course "Materials Science"

The task of studying materials science is to provide students with knowledge and skills [3]:

1) on the choice of optimal materials, which until recently in the learning process was solved by descriptive courses in materials science (information about existing, new materials being implemented and implemented; about structural transformations), accompanying heat treatment, at temperatures above the temperatures of machine parts caused by its operation);

2) to determine the ability of the material to increase the useful life and technological operation of industrial facilities, which is solved by studying structural transformations under the influence of numerous operational factors that determine the processes of destruction of the material. And the second topic is not sufficiently explained to students, which reduces the level of training.

The idea that all materials change their structure and mechanical properties in the process of their production, the manufacture of parts and the operation of parts should be the fundamental basis of materials science and should be explained when considering:

1) microstructures of alloys as the main factor of their strength and durability;
2) crystal structure of materials;
3) allotropic transformations occurring at various stages of thermal and other types of materials processing;
4) the appearance of defects in the crystal structure and their effect on the physical and mechanical properties of materials;
5) dislocation-structural mechanism of destruction;
6) the mechanism of cross-border structural transformations during deformation;
7) the influence of the microstructure of parts on the reliability of the machine during operation;
8) selection of material according to operating conditions.

Continuously increasing requirements for the properties of materials necessitate the advanced development of scientific developments in the field of materials science. Modern materials science as a science of the structure and properties of various materials is being significantly modernized due to the integration of solid state physics, chemistry and technology of inorganic substances, mechanics of solid body deformation and nonlinear fracture mechanics [4].

The content of the course "Materials Science" should be grouped around fundamental physical and scientific and technical theories, which makes it possible to realize the integrity of education.

2. Methods of teaching the course "Materials Science"

The methodological system of training should meet the didactic principles of scientific character, accessibility, continuity and continuity of training, interdisciplinary connections, etc.) and is mainly based on the principle of unity of fundamental and professional orientation of training.

Methods, forms and means of teaching are the ways to implement the goal and content.

Training methods should ensure the readiness of the future specialist not only to master certain knowledge, skills and abilities, but also to their continuous improvement, development of potential. Therefore, the question arises before any teacher: how, without destroying the integrity of the scientific discipline, to interest the student in in-depth study of the subject, the student's interest in in-depth study of the subject, assimilation of the maximum possible material, how to create a foundation for independent training? The priority methods are gnostic (problem presentation, partially-search, research, etc.), methods of self-management by educational actions (independent work of students, including the preparation of messages, abstracts on the most relevant and modern topics of the course.

The solution of the problem is impossible without understanding the basic concepts and knowledge that are formed in the learning process at lectures, laboratory and practical classes. Express tests (quizzes) and control works on the most important topics of the course are worked out at the "Department of Building Materials" of the Engineering University to improve the effectiveness of lectures and the timeliness of students' study [5]. So, at the opening of the lesson, the lecturer introduces the basic conditions of this method, which includes the following. After each lecture, the student should study the information on the abstract and the recommended main, additional reading. Based on the materials of this lecture, the student formulates and writes down in conclusion the ten most important, in his opinion, questions. At the next lecture, the lecturer checks the questions prepared by the students and notes the failed ones.

Students who have not prepared questions will work extra hours. Instead of repeating the material of the last lecture, there will be an express test (5-6 minutes of questionnaire) for students who have prepared questions for the last lecture. The lecturer calls the student and the question number. The student reads his question aloud, and the lecturer calls the student who answers this question. According to the answer, the student receives a grade. The student who asked the question can also answer. After the express test, the lecturer summarizes the results of the student's independent work on assimilating the information of the last lecture and gives a task for further study.

Preparatory work forces students to study new material more deeply, the student learns the terms and definitions of materials science more easily and acts confidently in the next lesson. Written test papers are worked out after meaningful lectures, about which students are informed in advance. For example, students and postgraduates of engineering and technical areas should easily navigate the phases and structural components of iron-carbon alloys – steels and cast iron. For them, this is possible only with knowledge and understanding of the "iron-cementite" ("iron-graphite") state diagram. To do this, in accordance with the working program of the course "Materials Science", "Diagrams of the state of binary alloys" are studied beforehand, then a connection is established between these diagrams and the diagram "iron-cementite" and the lecturer gives the task to independently and constructively understand the latter scheme [6]. After the lecture according to this scheme, the lecturer gives 5-7 days for independent work on its study and assigns the date of the control work. It usually lasts 20-25 minutes at the beginning of the next lecture and after laboratory work on the topic "Microstructural analysis of steel and cast iron". For a deeper understanding of the state diagrams of binary alloys, the lower edge of the "liquidus curve" is shaded, i.e. it is noted that the alloys below the liquidus curve are in a liquid-solid state. The lower edge of the "solidus curve" is marked with frequent strokes, which means that the alloys below this line are in a solid state. Similarly, the curves of secondary and tertiary crystallization are marked.

If the student remembers the scheme correctly, indicates all the fields of phases and structural components, transformation temperatures, carbon concentrations, states the material being studied, gives correct definitions of structural components, understands the material, can justify his opinion, can apply knowledge in practice, then the control work is considered completed. it is considered implemented. The student remembers this scheme for many years, which is necessary, first of all, for his further professional activity and only then for the successful completion of the test on the exam.

Such an active independent work of students is possible only if there is a serious and stable motivation. The most powerful motivating factor is the preparation for further effective professional activity. Hovewer, there are other factors that contribute to improving the student's independent work, these include:

1) The usefulness of the work performed. If a student knows that the knowledge, skills and abilities acquired in the classroom will be used in practice in the future, in a thesis (project) or for publication, then his attitude to the task changes for the better and its quality increases;

2) Participation of students in creative activities. This may be participation in the research or methodological work of the department;

3) Participation in research competitions, science days at the department, faculty, university, etc.;

4) The use of motivating factors of objective knowledge control (automated test control);

5) Awarding students for academic and creative achievements (scholarships, awards) and penalties for failure [7].

3. Methods of control of students' knowledge

In recent years, new information technologies have been increasingly used in the educational process; automated learning and control systems make it possible to independently study a particular course and simultaneously monitor the assimilation of educational material.

One of the main motivating factors for the activation of students' independent work on the subject is the presence of objective control of the volume and level of their knowledge. The solution to this problem is impossible without the use of automated testing control. When translating the course material into tests, an automated test control program is developed. The student solves problems randomly assigned by the computer from different sections of the discipline. The main problem is the ability of the teacher to choose the right form of the test, which more fully and correctly expresses the content of the educational material and objectively evaluates it.

There are four forms of tests [8]:

1) closed (multiple choice) is a form of assessment in which respondents are asked to choose the best possible answer (or answers) from the options from the list;

2) open is a form of assessment in which respondents are asked to recall the correct term (answer) and fill in the gap after this statement;

3) the matching task form, the test form, is widely used, where the correspondence of the elements of a set is determined by the elements of another set;

4) the sequence of certain actions, operations, etc.

Performing computer testing using all four of the above methods allows you to use illustrative material. For example: The ECD lines in Figure 1 are called transformation curves.

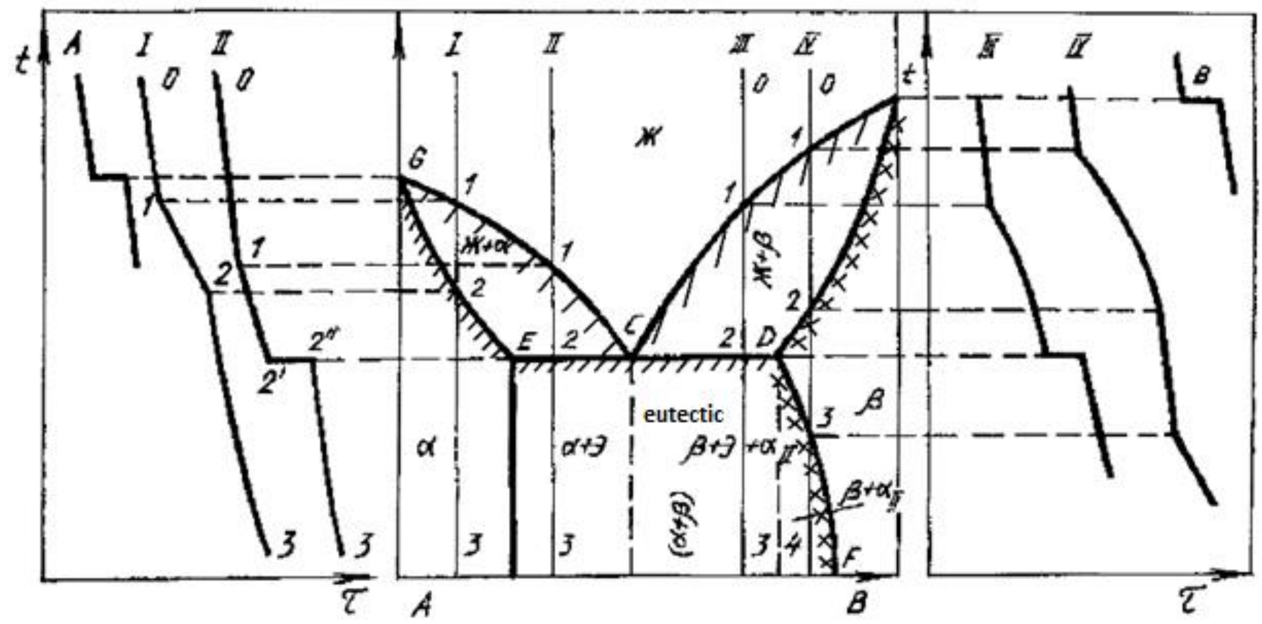

Fig.1. – Diagram of iron-cementite

The student types the word "eutectic" and gets a score if the answer is correct.

Example of the test according to the diagram "iron-cementite": Determine the correspondence of 1-7 (K1-K7) alloys (Fig. 2) to their names (a-k):

a) bronze;
b) technical cast iron;
c) brass;
d) zaeutectic cast iron;
e) pre-eutectic steel;
e) eutectic cast iron;
d) pre-eutectic cast iron;
h) ferrite;
i) hypereutectic steel;
k) eutectic steel.

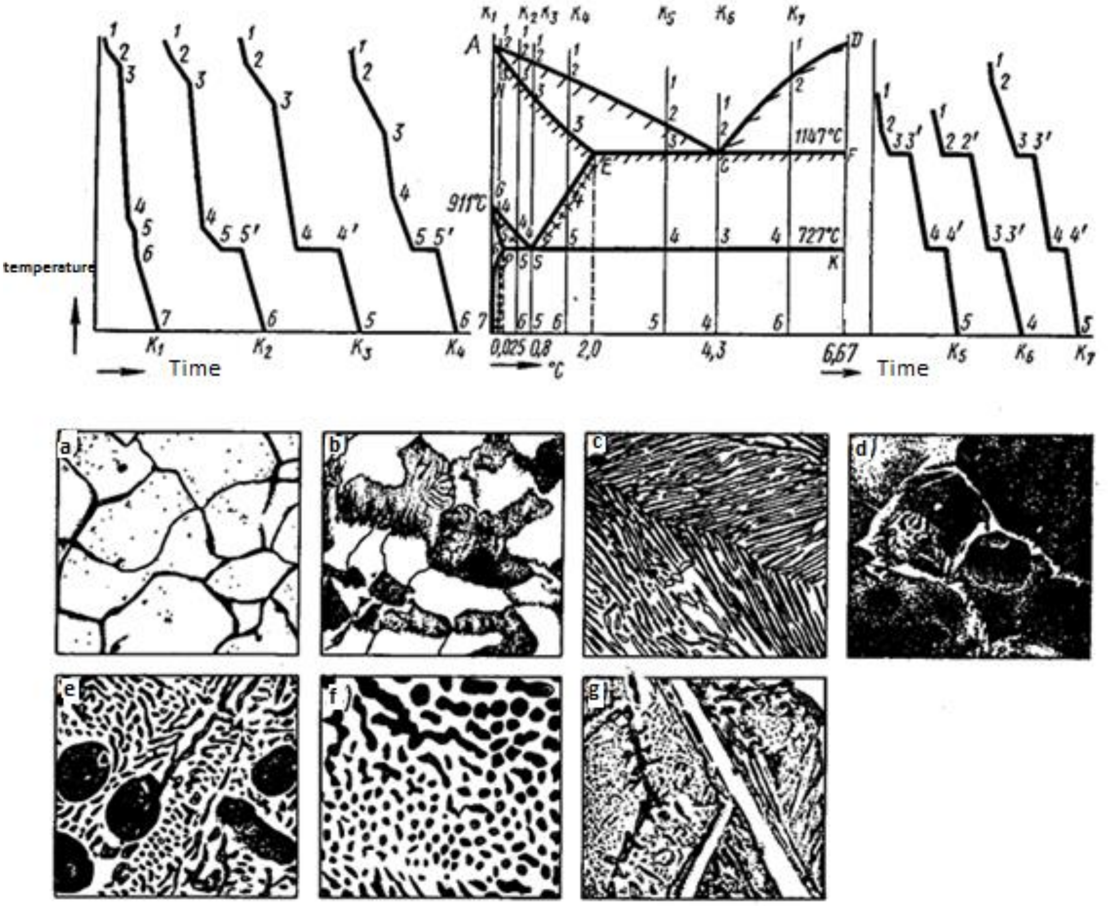

Fig.2. – Assignment for computer testing of students

The student sets the logical matching positions (K1-K7) (1-7) and names (a-k), enters the answer code into the computer, for example, 1b, 2d, 3k, etc., after which the computer program calculates the correct answers (plus) and incorrect answers (no answer, minus). For this task, a well-prepared student can get 7 points (100% correct answers). With less correct answers, its success ranges from 100% to 0% [2].

Innovations and computer testing methods for the course "Materials Science and Technology of building materials" were heard at the last four All-Russian conference of heads of the Department "Materials Science and Technology of Building Materials" [3]. Following the results of these conferences, the authors take an active part in creating a bank of test tasks and participate in the cabinet of "Interactive methods for monitoring the volume and level of knowledge of students" of the Ministry of Education and Science of the Russian Federation.

Conclusions

The means of teaching students in the classroom for the course "Materials Science" are tasks for lectures, laboratory, research work;

1) To implement a modern approach to the development of new materials and technologies, it is necessary to use computer testing methods in the educational process;

2) The selected components of the methodological system of teaching materials science can become the basis for the formation of modern knowledge about materials among students and contribute to the training of competent, highly qualified specialists in the field of materials science and mechanical engineering.

References

[1] Avanesov V.S. Formulation of test tasks. - M.: Adept, 1998. – 134 p.

[2] A.A. Smolkin, A.I. Batyshev, F.P. Khorokhorin. Estimation and realization of different tasks during computer testing // NOVIE TECHNOLOGII, MSOU, №3. 2007. – P. 45 - 48.

[3] Caturyan O.E., Smolkin A.A., Batyshev A.I. Methodical basis of development of automated testing control of students’ knowledge on materials science and technology of construction materials //Collection of materials of International conference of heads of materials science and technology of construction materials departments. – Saratov, SSTU, 2010. – P. 56 – 58.

[4] Pavlovych L., Bilous I. The concept of teaching methods, their classification //Sciences of Europe, № 51, (2020). – P. 9 – 12.

[5] Materials science and technology of construction materials test tasks /A.A. Smolkin, A.I. Batyshev, V.I. Bezpalko and etc.; edited by A.A. Smolkin – M.: Akademiya, 2011. – 67 p.

[6] Smolkin A.A. Innovations and problems of "Materials science and technology of construction materials" course/ / Izvestiya MGTU "MAMI". Peer-reviewed scholarly journal. Volume 2. Series – Engineering technology and materials, 2014. – P. 34 – 37.
[7] Leszek Adam Dobrzanski, Zbigniew Brytan, Brom Florian Teaching of material science matters using e-learning techniques //Archives of Materials Science and Engineering, 28(11), 2007. – P.691 – 694.
[8] Ovcharenkov E.A. Improvement of methods of checking and control of knowledge of students is one of the ways to improve the quality of the educational process //Modern problems of science and education, № 4, 2014. - P. 51 – 51.

Information of the author

Smolkin Alexander Alekseevich, candidate od technical sciences, professor of Moscow State University of Mechanical Engineering
E-mail: smolkin_a@mail.ru